TECHNICAL REPORT No. 19

A LOW ORDER BAROTROPIC MODEL ON THE SPHERE WITH OROGRAPHIC AND NEWTONIAN FORCING

by

E. Källén

July 1980

C O N T E N T S

ABSTRACT

An analysis of a low-order barotropic system with orographic and momentum forcing is presented. The low-order expansion of the streamfunction is performed on a spherical geometry, the expansion functions thus being spherical harmonics. Two purely zonal components and two wave components with the same zonal wavenumber but different orders, or latitudinal wavenumbers, are described by the model. The non-linear terms appearing in the six ODEs governing the time evolution of the system, give rise to bifurcations into multiple steady-state solutions.

In order to retain as many non-linear terms as possible, one must, however, be careful in the choice of components. An analysis of the different possibilities is presented and two examples having quite different properties are investigated. Three of the components are the same in each example, while the three others differ in their symmetry properties around the equator.

For the example which is believed to be most representative of realistic conditions, it is shown that a combination of orographic forcing and zonally asymmetric momentum forcing is required to obtain multiple steady-state solutions for realistic parameter values. The forcing must exceed certain critical values for a bifurcation from one to three steady-states to appear. A stability investigation of the steady state triplets shows that two are stable while one is unstable. Examining the energetics of the two stable steady-states for a situation which corresponds to a wintertime forcing pattern, it is shown that one of the stable steady states is much more zonal than the other. The non-zonal circulation is similar to a "blocked" flow. Another significant difference in the energetics between the two flow types is the direction of the energy transfer between zonal and eddy kinetic energy. Comparisons with observational studies of "blocked" and zonal flow confirms that this is a characteristic feature of the observed energetics.

1. INTRODUCTION

In recent years there has been a renewed interest in the study of low-order systems to gain some insight into non-linear mechanisms present in the atmosphere. The basic procedure used when studying a low-order system is to expand the space dependent quantities into a series of orthogonal functions and to truncate this expansion by just retaining a few components. Each component is thought of as representing a certain scale of motion and, by inserting the truncated expansion into an equation of motion, one can study the non-linear interactions between the scales considered. One thus neglects all interactions with spectral components outside the ones taken into account. This is of course a serious limitation of low-order systems, but it is nevertheless believed that a study of such systems is one way of getting an insight into the non-linear mechanisms present in the atmosphere.

When the orthogonal expansion is inserted into an equation governing the atmospheric fields of motion, the truncation cannot be made arbitrarily. This was first demonstrated by Lorenz (1960) for the barotropic vorticity equation on a β-plane and later by Platzmann (1962) for the same equation on a spherical domain. Lorenz obtained what he called a "maximum simplification" of the atmospheric equations of motion, because a further reduction of components would lead to a system with trivial non-linear interactions. Later, Lorenz (1962) used a low-order system to study forced behaviour of the flow in a rotating annulus for varying rates of heating and rotation. That study was very successful in describing theoretically the observed features of such a flow.

To study the effect of orographic forcing on the non-linear energy transfer between the larger scales of motion, Charney and de Vore (1979) (hereafter called CdV) extended Lorenz's (1960) barotropic β-plane model to include orographic forcing. With a minimal system they showed that for a given forcing it was possible for the flow to arrange itself in several equilibrium states, some stable and some unstable. Wiin-Nielsen (1979) studied a low-order barotropic model on the sphere and with only Newtonian forcing. He also obtained multiple steady-state solutions when the forcing exceeded a certain critical value. Trevisan and Buzzi (1980) recently studied the effect of orographic forcing on a non-dissipative, barotropic, β-plane channel model and obtained results similar to the ones described by CdV. They did, however, not expand the solution in trigonometric functions but instead they chose to expand the solution in terms of a small parameter, the ratio of the width to the length of the channel. Solving for the zero-th order streamfunction, they obtained an equation similar to the one of a forced non-linear oscillator. Combining the effects of orographic

and cyclonic vorticity forcing, Kalnay-Rivas and Merkine (1980) have recently shown that non-linear mechanisms can enhance the response downstream of the orography if there is a certain phase relationship between a cyclonic vorticity source and an isolated mountain. The flow patterns found for the large amplitude steady-state solutions of their β-plane, channel model strongly resemble atmospheric blocking.

In Trevisan and Buzzi's and CdV's studies, the multiplicity of steady states is associated with the resonance occurring when the Rossby wave, generated by the zonal flow over the orography, becomes stationary. Through the non-linear interaction between the zonal flow and the wave components of the flow and due to the orography, the components can arrange themselves in two stable equilibria, one close to resonance with a large amplitude wave and a weak zonal flow, the other with a strong zonal flow and a weaker wave component.

In the abovementioned studies the existence of the two stable equilibria were dependent on the resonance phenomena in a β-plane channel. It is the purpose of this study to investigate whether this result is also valid for a low-order model with a spherical geometry. We will also investigate the combined effects of orographic and Newtonian forcing.

The governing equation of the model used is the equivalent barotropic, quasi-geostrophic vorticity equation. Orographic forcing is introduced through a forced vertical velocity at the lower boundary while the Newtonian forcing acts as a momentum source/sink in the vorticity equation. After an expansion of the stream function and forcing fields in spherical harmonics, a low-order system is chosen which includes nonlinear interactions between all scales involved (Platzmann, 1962). The minimal system contains two purely zonal scales of motion and two wave components with the same zonal wave number but different latitudinal scales of motion. It is shown that a certain choice of components gives the same type of equations as the ones used by CdV, while other choices give systems of equations quite different from CdV's but more similar to the ones used by Wiin-Nielsen (1979). Both types of systems have multiple equilibria for certain combinations of orographic and Newtonian forcing but, for a choice of parameters believed to be realistic in representing conditions present on the Northern Hemisphere, it is demonstrated that the flow patterns obtained for the stable equilibria have some features which are different from the ones obtained by CdV. The energetics of the equilibria are also examined and compared to a case study by Wiin-Nielsen et al (1964) and Wiin-Nielsen (1965).

2. THE MODEL

In order to study the effects of orography and Newtonian forcing on atmospheric flow, we assume the flow to be governed by the quasi-geostrophic vorticity equation

$$\frac{\partial}{\partial t} \nabla^2 \eta + \underline{V} \cdot \nabla \ (\nabla^2 \eta + f) = f_o \frac{\partial \omega}{\partial p} - E \nabla^2 \eta + \nabla^2 \eta_E \qquad (1)$$

For an explanation of notation, see the list of symbols in Appendix I. The effect of the orography is introduced into the model by integrating (1) vertically assuming the atmosphere to be equivalent barotropic and taking the vertical velocity at the surface ($p = p_o$) to be given by

$$\omega_o \tilde{} - g \rho_o w_o = - g \rho_o \underline{V} \cdot \nabla m \qquad (2)$$

where m is the dimensional mountain height.

The equivalent barotropic model is obtained by assuming the vertical variation of the streamfunction, η, and the forcing, η_E, to be of the form

$$\begin{bmatrix} \eta \\ \eta_E \end{bmatrix} = A \ (p) \begin{bmatrix} \bar{\eta} \\ \bar{\eta}_E \end{bmatrix}$$

where the horizontal overbar denotes a vertical average. Integrating (1) vertically, inserting the vertical velocity given by (2) at the lower boundary and applying the integrated vorticity equation at the equivalent barotropic level p^* ($A(p^*) = A^2(p)$) we get,

$$\frac{\partial}{\partial t} \nabla^2 \eta^* + \underline{V} \cdot \nabla (\nabla^2 \eta^* + f + f_o \frac{A(p_o)}{A(p^*)} \frac{m}{H}) = - E \nabla^2 \eta^* + \nabla^2 \eta_E^* \qquad (3)$$

where a $(\ )^*$ denotes that the value is taken at the equivalent barotropic level, p^*.

By non-dimensionalizing (3) with the angular velocity and radius of the earth

$$\tau = \Omega t \qquad \psi = \frac{\eta^*}{a^2 \Omega} \qquad \zeta_E = \frac{1}{\Omega} \nabla^2 \eta_E^* \qquad \zeta = \frac{1}{\Omega} \nabla^2 \eta^*$$

$$\varepsilon = \frac{E}{\Omega}$$

and defining $h = 2 \mu_o \frac{A(p_o)}{A(p^*)} \frac{m}{H}$

we obtain

$$\frac{\partial \zeta}{\partial \tau} = J(\zeta + h, \psi) - 2 \frac{\partial \psi}{\partial \lambda} - \varepsilon \zeta + \zeta_E \tag{4}$$

which is the non-dimensional form of the governing equation used in this study.

2.1 Spectral representation

The main purpose is to investigate how the non-linearity present in the advection term $J(\zeta + h, \psi)$ in Eq. (4) affects the energy transfer between different scales of motion. We do this by determining the steady states of a spectrally truncated version of (4), and investigate their stability. The most interesting parameters to be varied are the mountain height, given by h, and the intensity as well as the phase (in relation to the mountains) of the Newtonian forcing, ζ_E. The spectral expansion is performed on a spherical domain, the expansion functions thus being spherical harmonics

Following the analysis given by Platzmann (1962), we write the vorticity, ζ, the mountains, h, and the Newtonian forcing, ζ_E, as a sum of spherical harmonics

$$\begin{pmatrix} \zeta \\ \zeta_E \\ h \end{pmatrix} = \sum_\gamma \begin{pmatrix} \zeta_\gamma \\ \zeta_{E,\gamma} \\ h_\gamma \end{pmatrix} P_\gamma(\mu)\, e^{ik_\gamma \lambda} \tag{5}$$

Here $P_\gamma(\mu)$ are the associated Legendre polynomials normalized so that

$$\frac{1}{2} \int_{-1}^{1} [P_\gamma(\mu)]^2 \, d\mu = 1 \tag{6}$$

and γ is the complex wavenumber, $\gamma = m_\gamma + ik_\gamma$. The zonal wavenumber of a component γ is given by k_γ while m_γ defines the order of the Legendre polynomial. By the definition of ζ we also have

$$\psi_\gamma = -\frac{1}{c_\gamma} \zeta_\gamma \tag{7}$$

where $c_\gamma = m_\gamma (m_\gamma + 1)$.

Inserting the expansion (5) into the non-dimensional barotropic vorticity equation (4), we obtain for each wavenumber γ

$$\frac{d\zeta_\gamma}{d\tau} = A_\gamma(\psi,\zeta) + A_\gamma(\psi,h) + 2\, ik_\gamma c_\gamma \zeta_\gamma - \varepsilon \zeta_\gamma + \zeta_{E,\gamma} \tag{8}$$

where the transport spectrum $A_\gamma(\psi,\zeta)$ is given by

$$A_\gamma(\psi,\zeta) = \frac{i}{2} \sum_{q,r} \left(\frac{1}{c_q} - \frac{1}{c_r}\right) I_{\gamma,q,r}\, \zeta_q\, \zeta_r \tag{9}$$

The summation over q and r (complex wavenumbers) is non-redundant, i.e. only distinct combinations of q and r occur.

Assuming the orography to be in only one spectral component, α, with the amplitude h_α, the interaction between the flow and the mountain may be written

$$A_\gamma(\psi,h_\alpha) = \frac{i}{2} \sum_{q} \left(I_{\gamma,q,\alpha} h_\alpha + I_{\gamma,q,\bar{\alpha}} \bar{h}_\alpha\right) \frac{\zeta_q}{c_q} \tag{10}$$

where an overbar denotes a complex conjugate. The so called interaction integrals, $I_{\gamma,q,r}$, appearing in (9) and (10) are defined

$$I_{\gamma,q,r} = \begin{cases} 0 \text{ if } k_\gamma \neq k_q + k_r \\ \displaystyle\int_{-1}^{1} P_\gamma \left(k_q P_q \frac{dP_r}{d\mu} - k_r P_r \frac{dP_q}{d\mu}\right) d\mu \text{ if } k_\gamma = k_q + k_r \end{cases} \tag{11}$$

It can be shown, as given by Platzmann (1962), that the integral appearing in (11) when $k_\gamma = k_q + k_r$ vanishes unless the following selection rules are satisfied for γ, q and r.

$$k_q^2 + k_r^2 \neq 0 \tag{12a}$$

$$|m_q - m_r| < m_\gamma < |m_q + m_r| \tag{12b}$$

$$m_q + m_r + m_\gamma \text{ is odd} \tag{12c}$$

$$q \neq r$$

$$\bar{q} \neq \gamma \text{ and } \bar{r} \neq \gamma \tag{12e}$$

When truncating the expansion for ζ, retaining only a few components, the selection rules give several restrictions on the choice of components if one wishes to retain some non-linear terms. Platzmann (1962) showed that in order to obtain active non-linear interactions between the components, one needs at least a three component system, i.e. one involving three complex wavenumbers. The complex conjugate of each component with $k \neq 0$ must also be included to describe the phase of the wave components.

The simplest three component system having active non-linear interactions is one in which one component is purely zonal, i.e. k = 0, and the two other components have the same non-zero wavenumber. In Platzmann's three component system, the purely zonal component with the complex wavenumber $\gamma = 1$ is implicitly included, as there are no non-linear flow interactions to this component. When orographic forcing is present, there may however be interactions involving the $P_1(\mu)$ component between the orography and the other flow components and consequently this component always has to be included. Physically the component with $\gamma = 1$ can be seen as giving rise to a zonal flow with constant angular velocity. In the conservative case without forcing this can be taken care of with a suitable coordinate transformation. In the forced case, the coordinate system has to have a fixed relation to the forcing, thus the component with $\gamma = 1$ has to be included.

The choice of components in the special case of a three component system that we want to consider here can thus be summarized as in Fig. 1.

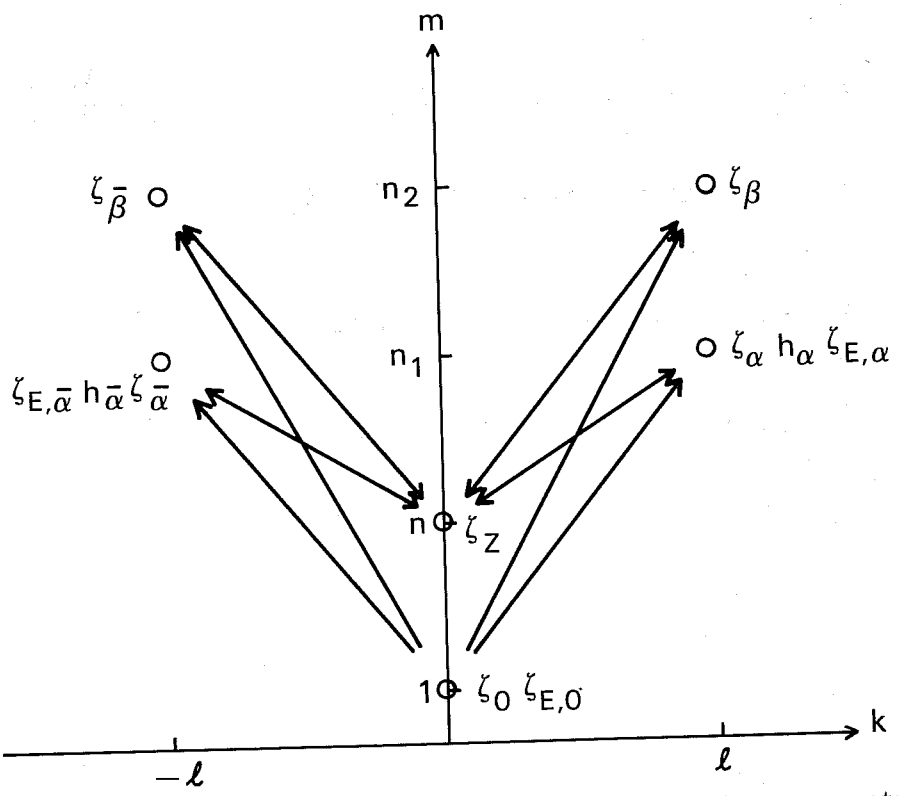

Fig. 1 Representation in the wave number plane of the components used in the model. The horizonal axis gives the zonal wave number, k, while the vertical axis gives the order, or latitudinal wavenumber, m of the Legendre functions.

The notation adopted in Fig. 1 for the wavenumbers α and β implies

$$\alpha = n_1 + i\ell \qquad \beta = n_1 + i\ell$$

Orography is included in only one component, α, while Newtonian forcing is assumed to be present in the wave component α and the purely zonal component with $m = 1$. Orography is thus present in only one wave component while there is both a zonal and a zonally asymmetric momentum forcing, the latter being in the same wave component as the orography. Using (8) we can now write our truncated model as a system of ordinary differential equations in the time dependent variables ζ_o, ζ_n, ζ_α and ζ_β

$$\frac{d\zeta_o}{d\tau} = i\frac{\sqrt{3}}{2}\ell(\bar{\zeta}_\alpha h_\alpha - \zeta_\alpha \bar{h}_\alpha) - \varepsilon\zeta_o + \zeta_{o,E}$$

$$\frac{d\zeta_n}{d\tau} = \frac{i\ell}{2}\left[I\left(\frac{1}{c_1} - \frac{1}{c_2}\right)(\bar{\zeta}_\alpha \zeta_\beta - \zeta_\alpha \bar{\zeta}_\beta) + I(\bar{\zeta}_\beta h_\alpha - \zeta_\beta \bar{h}_\alpha) + I_1(\bar{\zeta}_\alpha h_\alpha - \zeta_\alpha \bar{h}_\alpha)\right]$$

$$- \varepsilon\zeta_n \qquad (13)$$

$$\frac{d\zeta_\alpha}{d\tau} = \frac{i\ell}{2}\left[I_1\left(\frac{1}{c_1} - \frac{1}{c}\right)\zeta_\alpha\zeta_n + I\left(\frac{1}{c_2} - \frac{1}{c}\right)\zeta_\beta \zeta_n - h_\alpha\left(\sqrt{3}\,\zeta_o + \frac{I_1}{2}\zeta_n\right)\right]$$

$$- i\ell\left(2\zeta_\alpha - \left(\frac{1}{c_1} - \frac{1}{2}\right)\sqrt{3}\,\zeta_\alpha\zeta_o\right) - \varepsilon\zeta_\alpha + \zeta_{\alpha,E}$$

$$\frac{d\zeta_\beta}{d\tau} = \frac{i\ell}{2}\left[I_2\left(\frac{1}{c_2} - \frac{1}{c}\right)\zeta_\beta \zeta_n + I\left(\frac{1}{c_1} - \frac{1}{c}\right)\zeta_\alpha \zeta_n - \frac{I}{2}h_\alpha \zeta_n\right]$$

$$- i\ell\left(2\zeta_\beta - \left(\frac{1}{c_2} - \frac{1}{2}\right)\sqrt{3}\,\zeta_\beta\zeta_o\right) - \varepsilon\zeta_\beta$$

where the three different interaction integrals appearing are

$$I = \int_{-1}^{1} P_{n_1}^{\ell} P_{n_2}^{\ell} \frac{dP_n}{d\mu}\, d\mu \qquad (14a)$$

$$I_1 = \int_{-1}^{1} (P_{n_1}^{\ell})^2 \frac{dP_n}{d\mu}\, d\mu \qquad (14b)$$

$$I_2 = \int_{-1}^{1} (P_{n_2}^{\ell})^2 \frac{dP_n}{d\mu}\, d\mu \qquad (14c)$$

and $c = n(n+1)$, $c_1 = n_1(n_1+1)$, $c_2 = n_2(n_2+1)$

The interaction integral I appears in front of terms describing interactions between the zonal component ζ_n, the wave component ζ_α and the wave component ζ_β. Interactions between ζ_n, ζ_α and $\zeta_{\bar{\alpha}}$ involve I_1 while the interactions between ζ_n, ζ_β and $\zeta_{\bar{\beta}}$ involve I_2. The system thus only describes interactions between wave components and the zonal component ζ_n, no wave-wave to wave interactions are possible in this low-order system. A pictorial representation of the non-linear interactions within the system, is given by the arrows in Fig. 1.

In order to find the steady states of this system and their stability properties more easily, we convert the system (13) into six equations in the real domain. At the same time, we convert the vorticity amplitudes of each component into stream function amplitudes with the aid of Eq. (7). Thus we define the real amplitudes of the stream function to be

($u_o > 0$ for westerlies in the Northern Hemisphere)

$$u_o = \zeta_o/2 \tag{15a}$$

$$z = \zeta_n/c \tag{15b}$$

$$x_1 = -(\zeta_\alpha + \zeta_{\bar{\alpha}})/c_1 \tag{15c}$$

$$y_1 = -\,i(\zeta_\alpha - \zeta_{\bar{\alpha}})/c_1 \tag{15d}$$

$$x_2 = -\,(\zeta_\beta + \zeta_{\bar{\beta}})/c_2 \tag{15e}$$

$$y_2 = -\,i(\zeta_\beta - \zeta_{\bar{\beta}})/c_2 \tag{15f}$$

and the truncated expansion of the stream function in terms of the real coefficients becomes

$$\begin{aligned}\psi(\mu, \lambda, \tau) &= -\,u_o(\tau)\, P_1(\mu) + z(\tau)\, P_n(\mu) + \\ &+ (x_1(\tau) \cos \ell\lambda + y_1(\tau) \sin \ell\lambda)\, P^{\ell}_{n_1}(\mu) + \\ &+ (x_2(\tau) \cos \ell\lambda + y_2(\tau) \sin \ell\lambda)\, P^{\ell}_{n_2}(\mu)\end{aligned} \tag{16}$$

A similar expansion holds for ψ_E while the orography, h, is assumed to be given by

$$h = h_1 \cos \ell\lambda\, P^{\ell}_{n_1}(\mu) \tag{17}$$

Inserting (15), (17), and the corresponding expressions for ψ_E into Eq. (13), we obtain

$$\begin{cases} \dot{u}_o = & & h_1\delta_1 y_1 & -\varepsilon u_o + u_{oE} \\ \dot{z} = \gamma_1 (x_2 y_1 - x_1 y_2) & & -h_1(\delta_2 y_2 + \delta_3 y_1) & -\varepsilon z \\ \dot{x}_1 = \gamma_2 z y_2 + \gamma_4 z y_1 - \alpha_1 u_o y_1 + \beta_1 y_1 & & & -\varepsilon x_1 + x_{1E} \\ \dot{y}_1 = -\gamma_2 z x_2 - \gamma_4 z x_1 + \alpha_1 u_o x_1 - \beta_1 x_1 & & +h_1(\delta_5 z - \delta_4 u_o) & -\varepsilon y_1 + y_{1E} \\ \dot{x}_2 = \gamma_3 z y_1 + \gamma_5 z y_2 - \alpha_2 u_o y_2 + \beta_2 y_2 & & & -\varepsilon x_2 \\ \dot{y}_2 = -\gamma_3 z x_1 - \gamma_5 z x_2 + \alpha_2 u_o x_2 - \beta_2 x_2 & & +h_1\delta_6 z & -\varepsilon y_2 \end{cases} \tag{18}$$

where

$$\alpha_1 = \sqrt{3}\ell\ (1 - \frac{2}{c_1}),\ \alpha_2 = \sqrt{3}\ell\ (1 - \frac{2}{c_2}),\ \beta_1 = \frac{2\ell}{c_1},\ \beta_2 = \frac{2\ell}{c_2}$$

$$\gamma_1 = \frac{I\ell}{4c}(c_2 - c_1),\ \gamma_2 = \frac{I\ell}{2c_1}(c_2 - c),\ \gamma_3 = \frac{I\ell}{2c_2}(c_1 - c)$$

$$\gamma_4 = \frac{I_1\ell}{2c_1}(c_1 - c),\ \gamma_5 = \frac{I_2\ell}{2c_2}(c_2 - c) \tag{19}$$

$$\delta_1 = \frac{\sqrt{3}}{4}\ell,\ \delta_2 = \frac{I\ell}{4c}, \delta_3 = \frac{I_1\ell}{4c},\ \delta_4 = \frac{\sqrt{3}\ell}{c_1},\ \delta_5 = \frac{I_1\ell}{2c_1}, \delta_6 = \frac{I\ell}{2c_2}$$

Without forcing and dissipation, the system described by Eqs. (18) is both energy and enstrophy conserving. If only orographic forcing is included, the system is conserving energy but not enstrophy.

2.2 Choice of components

Before continuing with an investigation of the steady states and stability properties of Eqs. (18), one must decide which associated Legendre polynomials to choose when evaluating the interaction integrals given by (14) and the coefficients given by (19). For certain choices of components the interaction integrals will vanish and one has to be careful in order to fulfill the selection rules given by (12) for at least one of the interaction integrals.

Through the symmetry properties of the Legendre polynomials, it is clear that if n is even, both I_1 and I_2 will vanish. If, on the other hand, n is odd, I_1 and I_2 are non-zero. For the interaction integral I to be non-vanishing, we must require that the sum $n + n_1 + n_2$ is odd according to selection rule (12c). These results are summarised in Fig. 2 where all possible combinations of n, n_1 and n_2 are listed.

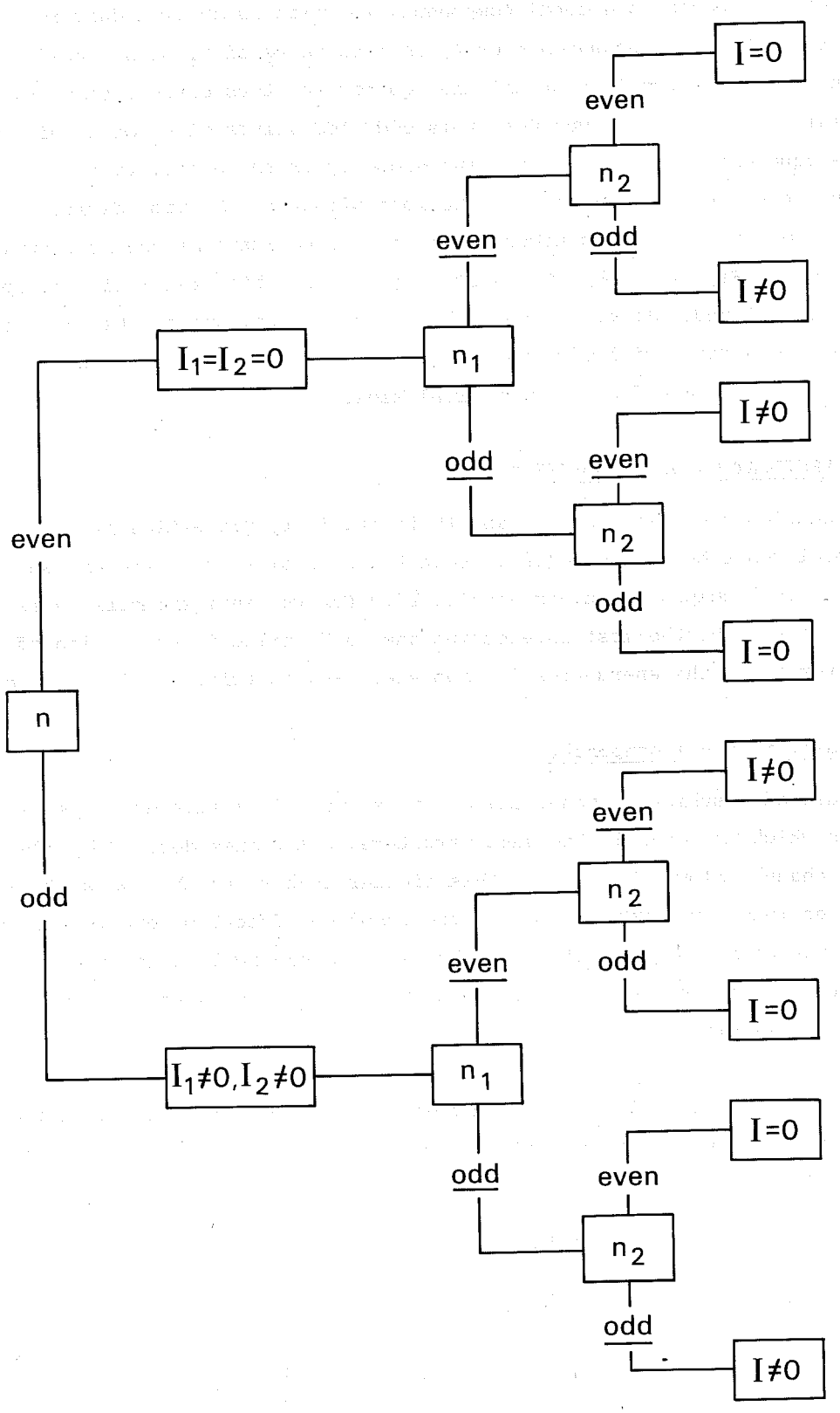

Fig. 2 A list of all possible combinations of even and odd values of n, n_1 and n_2. Using selection rule(12c) conclusions may be drawn regarding the values of the interaction integrals I, I_1 and I_2 as indicated in the figure. Underlined combinations are those which give a non-zero value of I.

An even n corresponds to a zonal component, z, which is an even function around the equator. For an even wavenumber ℓ, an even value of n_1 or n_2 implies a wave component which is symmetric around the equator and thus gives rise to cross-equatorial flow. If the wavenumber ℓ is odd, odd values of n_1 or n_2 give rise to cross equatorial flow. An important property of the system is that in order to include non-linear flow-flow interactions affecting the time derivative of the zonal component z, it is necessary to have I non-zero as can be seen from Eqs. (18). In Fig. 2, combinations of n, n_1 and n_2 which result in I being non-zero are underlined. It can be seen that if n is even, one of the wave components must have cross-equatorial flow while if n is odd, it is always possible to choose n_1 and n_2 so as to avoid cross-equatorial flow.

3. INVESTIGATION OF STEADY STATES

In this section the steady states and their stability properties are investigated for a model described by Eqs. (18). Both the case of a symmetric and an anti-symmetric zonal component, z, is considered. For the anti-symmetric case, which will turn out to be the most interesting one, a detailed investigation of the flow patterns and the energetics for two steady-state triplets will be presented.

3.1 Symmetric zonal component

In the case of a symmetric zonal component, z, we will arrive at a system of equations which have exactly the same structure as the ones derived by CdV for a β-plane, channel flow. Because of this similarity between the two systems we will not go into any detail regarding the combined effects of orographic and wave momentum forcing. We will only show the mathematical method used to analyse the bifurcation properties. The same method will be used later in a more complicated example.

If n is even, both I_1 and I_2 vanish and we must choose n_1 and n_2 so that one is even while the other is odd in order to assure that I is non-zero. The system of Eqs. (18) now becomes

$$
\begin{cases}
\dot{u}_o = & & \delta_1 h_1 y_1 & & - \varepsilon u_o + u_{oE} \\
\dot{z} = \gamma_1 (x_2 y_1 - x_1 y_2) & - \delta_2 h_1 y_2 & & & - \varepsilon z \\
\dot{x}_1 = \gamma_2 z y_2 & - \alpha_1 u_o y_1 & & + \beta_1 y_1 & - \varepsilon x_1 + x_{1E} \\
\dot{y}_1 = -\gamma_2 z x_2 & + \alpha_1 u_o x_1 & - \delta_4 h_1 u_o & - \beta_1 x_1 & - \varepsilon y_1 + y_{1E} \\
\dot{x}_2 = \gamma_3 z y_1 & - \alpha_2 u_o y_2 & & + \beta_2 y_2 & - \varepsilon x_2 \\
\dot{y}_2 = -\gamma_3 z x_1 & + \alpha_2 u_o x_2 & + \delta_6 h_1 z & - \beta_2 x_2 & - \varepsilon y_2
\end{cases}
\tag{20}
$$

and this system is, apart from the numerical values of the constants, exactly the same as the one derived and studied by CdV for a β-plane, channel flow. We notice that, as in CdV, if z, x_2 and y_2 are zero initially they will remain zero and excluding the Newtonian forcing in the wave components, the system may be written

$$\begin{cases} \dot{u}_o = \delta_1 h_1 y_1 - \varepsilon u_o + u_{oE} \\ \dot{x}_1 = -\alpha_1 u_o y_1 + \beta_1 y_1 - \varepsilon x_1 \\ \dot{y}_1 = \alpha_1 u_o x_1 - \delta_4 h_1 u_o - \beta_1 x_1 - \varepsilon y_1 \end{cases} \tag{21}$$

Solving for the steady states of the system given by (21), we arrive at the following equation in u_o

$$u_o^3 - u_o^2 \left(\frac{u_{oE}}{\varepsilon} + \frac{2\beta_1}{\alpha_1}\right) + \frac{u_o}{\alpha_1^2}\left[\delta_1\delta_4 h_1^2 + \varepsilon^2 + \beta_1^2 + 2\beta_1\alpha_1 \frac{u_{oE}}{\varepsilon}\right] = \frac{u_{oE}}{\varepsilon}\frac{(\varepsilon^2 + \beta_1^2)}{\alpha_1^2} \tag{22}$$

which also may be written

$$\frac{u_{oE}}{\varepsilon} = \frac{\delta_1\delta_4 h_1^2 u_o}{\varepsilon^2 + (\beta_1 - \alpha_1 u_o)^2} + u_o \tag{23}$$

The polynomial form (22) of the steady-state equation shows that we can at the most have three steady states for certain values of the forcing parameters. The other form of the steady-state equation, (23) allows us to investigate by graphical methods how the number of steady states varies with the forcing parameters.

The example chosen to illustrate this is one in which $\ell = 2$, $n = 2$ and $n_1 = 3$. The latitudinal structure of these components is given in Fig. 3. Fig. 4 is a plot of the curves given by Eq.(23) for some values of h_1. On the horizontal axes, u_o is plotted in units of m/s corresponding to the windspeed of the u_o-component at 45^o latitude. The vertical axes is also given in units of m/s at 45^o latitude corresponding to the purely linear response in u_o for a given forcing, u_{oE}.

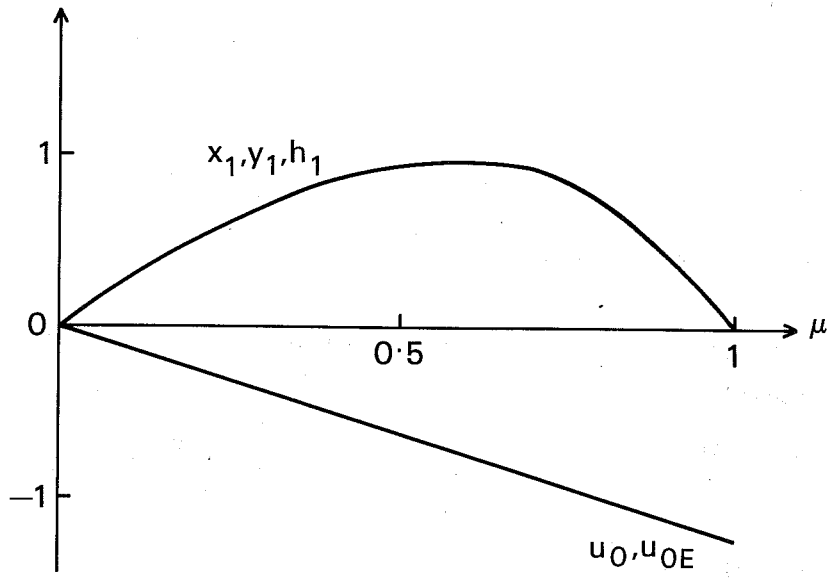

Fig. 3 Latitudinal structure of the components considered in the case of a symmetric zonal component, z. The horizontal axis gives latitude, μ, while the vertical axis gives the normalized amplitude of the Legendre functions.

The curve in Fig. 4 for $h_1 = 0$ is thus a straight line but for increasing values of h_1 we obtain a family of curves having both maxima and minima. As an example of a bifurcation a straight line is drawn for $\frac{u_{0E}}{\varepsilon}$ equal to 150 m/s. This line intersects the curve for $h_1 = 0.25$ three times and it is thus possible to have three steady-states for these values of the forcing parameters. An investigation of the eigenvalues to Eq. (21), linearized around a steady state, gives stability properties as indicated by full (stable) and dashed (unstable) lines in Fig. 4. The bifurcation from one to three steady-states occurs for a value of h_1 somewhere between 0.10 and 0.15.

The stability of the steady states given by (23) with respect to perturbations of z, x_2 and y_2 ("second mode perturbations") will of course be the same as in CdV, but if we choose n_1 to be odd, n_2 has to be even in order to preserve the non-linear interactions and this implies cross-equatorial flow in the x_2 and y_2 components. It is not believed that cross-equatorial flow has any significant effect on the atmospheric behaviour that we wish to describe with this very crude model and it would, therefore, be preferable to exclude all wave components

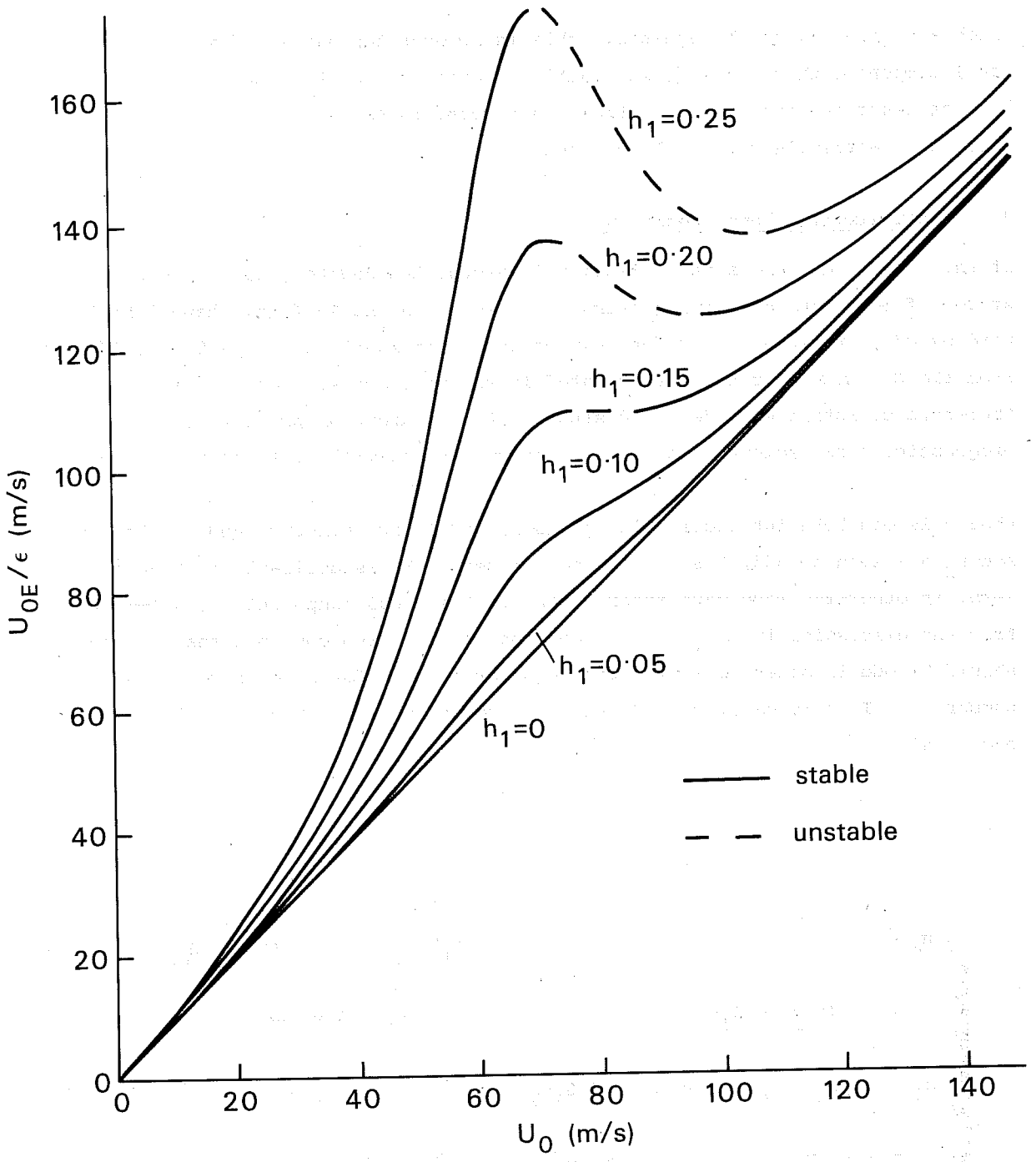

Fig. 4 Illustration of the bifurcation properties for variations of the forcing parameters in the case of a symmetric zonal component. Momentum forcing is acting on the zonal component with amplitude u_o while orography is present in only one wave component. The horizontal axis gives the amplitude of the u_o-component at a steady state in terms of the flow velocity at 45° latitude in m/s. The vertical axis gives the zonal forcing divided by the dissipation rate, which is the linear streamfunction response to the forcing in the absence of mountains. The forcing is thus also given in m/s at 45° latitude. Each curve corresponds to steady states for a certain value of the orographic parameter, h_1. Numerical evaluation of the eigenvalues for each steady state give stability properties as indicated by full lines (stable) and dashed lines (unstable). For further explanations, see text.
Parameter values: $\varepsilon = 0.1$, $H = 8$ km, $\Omega = 7.29 \cdot 10^{-5} s^{-1}$,
$a = 6.37 \cdot 10^6$ m, $\mu_o = 0.71$

which are non-zero at the equator. This is however impossible if we choose a zonal component which is an even function around the equator and we wish to have at least one interaction integral non-zero, so therefore we now turn to the case of an antisymmetric zonal component.

3.2 Antisymmetric zonal component

If the zonal component z is antisymmetric around the equator, we arrive at a system of equations containing terms not present in the β-plane, channel model used by CdV. We should therefore expect that this model has properties different from the CdV model (or the case treated in the previous section) and we will therefore go into a more detailed study of the bifurcation properties. Both orographic, zonal momentum and wave momentum forcing will be taken into account.

When n is odd both interaction integrals I_1 and I_2 are non-zero and, if both n_1 and n_2 are even or odd, I will also be non-zero. It is desirable to have I non-zero, as otherwise wave-wave interactions to the zonal component z are impossible. From the discussion in the previous section, we may also conclude that n_1 and n_2 should be odd in order to avoid cross-equatorial flow for an even zonal wave-number, ℓ. In this case, we have the full equations (18) which we will write here once again.

$$
\begin{cases}
\dot{u}_o = & & h_1\delta_1 y_1 & -\varepsilon u_o + u_{oE} \\
\dot{z} = \gamma_1 (x_2 y_1 - x_1 y_2) & & -h_1(\delta_2 y_2 + \delta_3 y_1) - \varepsilon z & \\
\dot{x}_1 = \gamma_2 z y_2 + \gamma_4 z y_1 - \alpha_1 u_o y_1 + \beta_1 y_1 & & & - \varepsilon x_1 + x_{1E} \\
\dot{y}_1 = - \gamma_2 z x_2 - \gamma_4 z x_1 + \alpha_1 u_o x_1 - \beta_1 x_1 & + h_1(\delta_5 z - \delta_4 u_o) & & - \varepsilon y_1 + y_{1E} \\
\dot{x}_2 = \gamma_3 z y_1 + \gamma_5 z y_2 - \alpha_2 u_o y_2 + \beta_2 y_2 & & & - \varepsilon x_2 \\
\dot{y}_2 = - \gamma_3 z x_1 - \gamma_5 z x_2 + \alpha_2 u_o x_2 - \beta_2 x_2 & + h_1\delta_6 z & & - \varepsilon y_2
\end{cases}
\tag{24}
$$

This system cannot be decomposed into two three-equation systems as in the previous case because of the term $- h_1 \delta_3 y_1$ in the $\dot{z}$-equation. We thus have to take all six components into account when solving for the steady states.

To solve for the steady states, we first notice that the equations for $\dot{x}_1$, $\dot{y}_1$, $\dot{x}_2$ and $\dot{y}_2$ are linear in x_1, y_1, x_2 and y_2. With the time derivatives set equal to zero, we can write this as a linear system of equations,

$$\underline{\underline{A}} \cdot \underline{B} = \underline{C} \tag{25}$$

where

$$\underline{\underline{A}} = \begin{pmatrix} -\varepsilon & -(\alpha_1 u_o - \beta_1 - \gamma_4 z) & 0 & \gamma_2 z \\ \alpha_1 u_o - \beta_1 - \gamma_4 z & -\varepsilon & -\gamma_2 z & 0 \\ 0 & \gamma_3 z & -\varepsilon & \beta_2 - \alpha_2 u_o + \gamma_5 z \\ -\gamma_3 z & 0 & -(\beta_2 - \alpha_2 u_o + \gamma_5 z) & -\varepsilon \end{pmatrix}$$

$$\underline{B} = \begin{pmatrix} x_1 \\ y_1 \\ x_2 \\ y_2 \end{pmatrix} \quad \text{and} \quad \underline{C} = \begin{pmatrix} -x_{1E} \\ h_1(\delta_4 u_o - \delta_5 z) - y_{1E} \\ 0 \\ -h_1 \delta_6 z \end{pmatrix}.$$

From Eq. (25) we can solve for x_1, y_1, x_2 and y_2 as functions of u_o and z. By inserting these solutions into $\dot{u}_o = 0$ and $\dot{z} = 0$ we obtain two simultaneous non-linear equations in u_o and z. By solving the equation $\dot{z} = 0$ for u_o and substituting the(se) value(s) in $\dot{u}_o = 0$, we finally arrive at one equation in z which may be analysed by graphical methods.

The example which will be analysed in detail here is one which tries to resemble the conditions present in the Northern Hemisphere. We assume a mountain and Newtonian forcing in the component P_3^2. The zonal component z is chosen to be in P_3^o while the second wave component with amplitudes in x_2 and y_2 is assumed to be in P_5^2. The latitudinal structure of these components is given in Fig. 5. This choice of components excludes cross-equatorial flow and simplifies the equations (24) somewhat because in this case $\gamma_3 = \gamma_4 = 0$. Note here that the u_o, x_1 and y_1 components are the same as the ones used in the case of a symmetric zonal component z in Section 3.1.

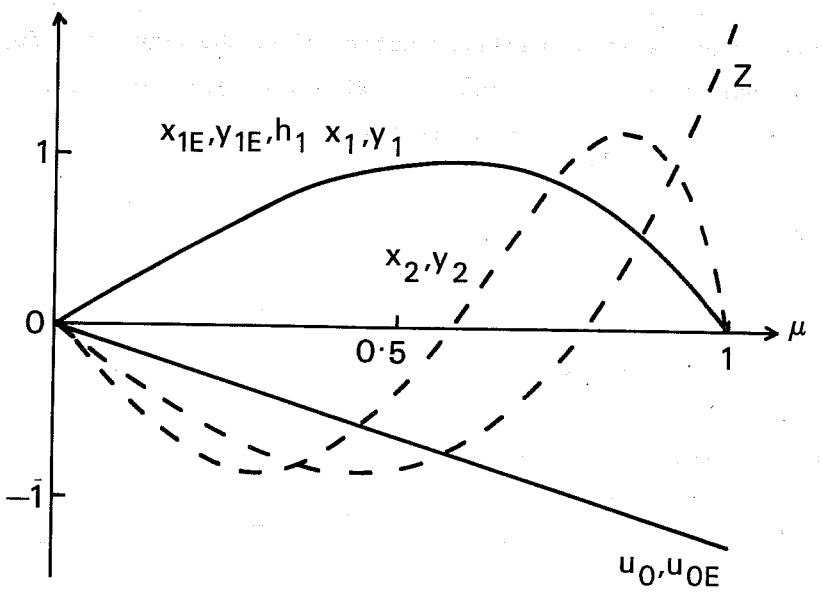

Fig. 5 As Fig. 3, but here for the case of an asymmetric zonal component, z.

Solving for the steady-state values of x_2 and y_2 we find

$$\begin{cases} x_2 = \dfrac{\delta_6 h_1 z\ (\gamma_5 z + \beta_2 - \alpha_2 u_o)}{\varepsilon^2 + (\gamma_5 z + \beta_2 - \alpha_2 u_o)^2} \\ \\ y_2 = \dfrac{\delta_6 h_1 z \varepsilon}{\varepsilon^2 + (\gamma_5 z + \beta_2 - \alpha_2 u_o)^2} \end{cases} \tag{26}$$

and for x_1 and y_1 we have

$$\begin{cases} x_1 = \dfrac{\varepsilon (x_{1E} + \gamma_2 z\ y_2) + (\alpha_1 u_o - \beta_1)(\delta_4 h_1 u_o - \delta_5 h_1 z - y_{1E} + \gamma_2\ z x_2)}{\varepsilon^2 + (\alpha_1 u_o - \beta_1)^2} \\ \\ y_1 = \dfrac{-\varepsilon (\delta_4 h_1 u_o - \delta_5 h_1 z - y_{1E} + \gamma_2 z x_2) + (\alpha_1 u_o - \beta_1)(x_{1E} + \gamma_2 z y_2)}{\varepsilon^2 + (\alpha_1 u_o - \beta_1)^2} \end{cases} \tag{27}$$

Notice the term $(\alpha_1 u_o - \beta_1)$ in the denominator of (27). We still have a resonance in the forced wave component for $u_o = \beta_1/\alpha_1$ as in the symmetric zonal component case.

To analyse the bifurcation properties of this system we plot u_{oE}/ε as a function of z with the aid of the equation $\dot{u}_o = 0$. The zonal component u_o is given as a function of z by solving the equation $\dot{z} = 0$. As this equation is non-linear in u_o, there may be multiple values of u_o for one z-value which will give several branches of the curve u_{oE}/ε (z).

3.2.1 Forcing by orography alone

For the purely orographically forced case, the result is shown in Fig. 6a. It is seen that for the mountain parameter $h_1 \leqslant 0.3$ only one steady state exists and a numerical evaluation of the corresponding eigenvalues has shown that this steady state is always stable. For higher mountains than 30% of the scale height and fairly large values of the zonal forcing a bifurcation from one stable to two stable and one unstable steady states occurs. The unstable steady states are given by the dashed curve in Fig. 6a. Comparing these bifurcation properties with the ones found for the earlier case involving only three components (which are the same as the z, x_1 and y_1 components in this case) one finds that the mountain height required for the bifurcation from one to three steady states is about twice as high. The zonal forcing required is about the same, still very high. An example of the stable flow field obtained for forcing below the bifurcation point is shown in Fig. 6b.

3.2.2 Forcing by momentum sources/sinks alone

Taking the mountain height h_1 equal to zero and only forcing the system with a momentum source/sink in the u_o and x_1 components, one may solve for the steady state(s) analytically. By equation (26) we find that x_2 and y_2 must be zero and, using the equation for $\dot{z} = 0$ (taken from (24)), we also find z to be zero. The zonal component u_o is only dependent on the zonal forcing u_{oE}, while the two forced wave components are given by

$$x_1 = x_{1E} \frac{\varepsilon}{\varepsilon^2 + (\beta_1 - \alpha_1 \frac{u_{oE}}{\varepsilon})^2}$$

$$y_1 = x_{1E} \frac{-(\beta_1 - \alpha_1 \frac{u_{oE}}{\varepsilon})}{\varepsilon^2 + (\beta_1 - \alpha_1 \frac{u_{oE}}{\varepsilon})^2} \qquad (28)$$

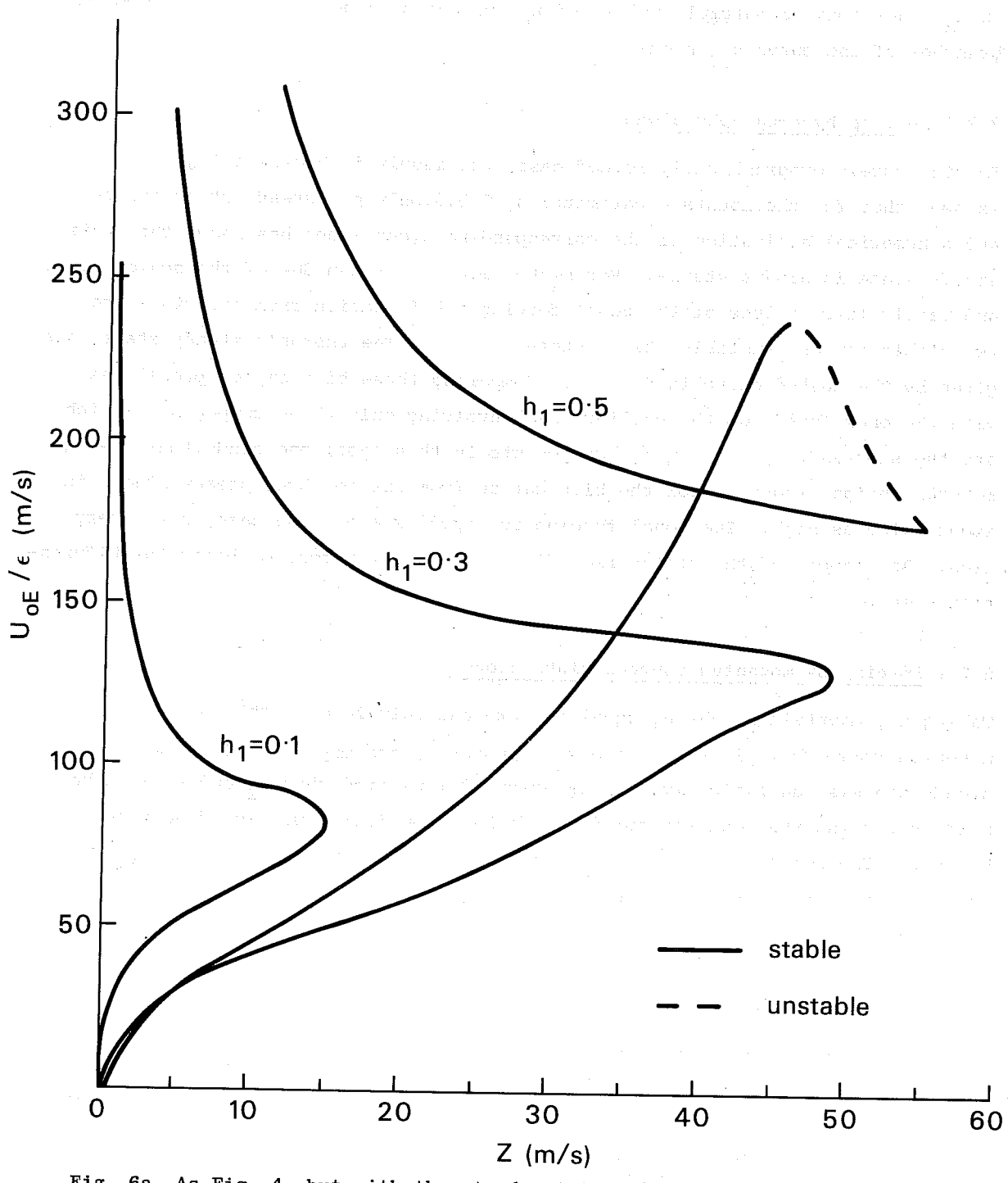

Fig. 6a As Fig. 4, but with the steady state value of z on the horizontal axis and z being an antisymmetric function around the equator.

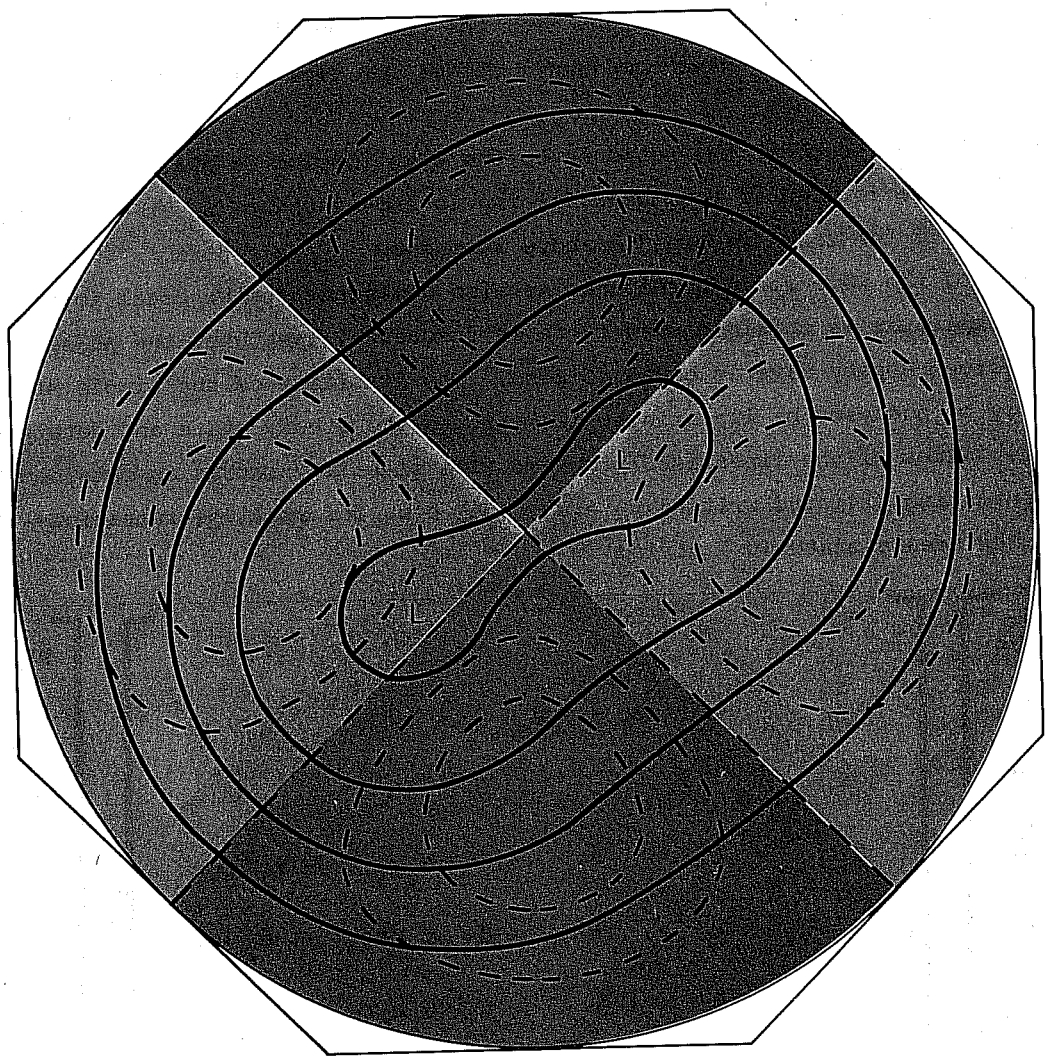

Fig. 6b Flow pattern obtained for a stable steady state with $h_1 = 0.1$, $\frac{u_{oE}}{\varepsilon} = 70$ m/s.
Full lines are isopleths for the streamfunction, dashed lines are isopleths for the orography. Areas with the orography above its mean value ("land areas") are green, while areas with the orography below its mean value ("oceans") are blue.

As there is no orography the phase of the Newtonian forcing is irrelevant and y_{1E} is set to zero. We thus have only one steady state in this case. Comparing this with the study by Wiin-Nielsen (1979) one finds that in his case it was possible to find multiple steady states for momentum forcing in only one of the wave components. This result is due to the fact that he is considering the case of a symmetric zonal component and the type of flow pattern described by his choice of components is different from the case considered here. In particular, his choice of wave components allows for flow across the equator.

From Eq. (28) we see that the response to the wave forcing is phase shifted to the west of the forcing if the zonal forcing is sub-resonant ($u_{oE}/\varepsilon < \beta_1/\alpha_1$), to the east if the zonal forcing is above resonance ($u_{oE}/\varepsilon > \beta_1/\alpha_1$). The amplitude of the wave forcing response is also dependent on the zonal forcing, maximum amplitude is obtained when there is resonance, i.e. when the phase speed of the forced Rossby wave is equal to zero. The stability of the single steady state may be analysed by linearising (24) around the steady state and determining the eigenvalues of the linearised problem. The stability matrix is obtained by differentiating (24) and writing $u_o = \bar{u}_o - \delta u_o$ etc. for small perturbations (δu_o) around the steady state ($\bar{u}_o$) giving

$$\begin{bmatrix} \delta\dot{u}_o \\ \delta\dot{x}_1 \\ \delta\dot{y}_1 \\ \delta\dot{z} \\ \delta\dot{x}_2 \\ \delta\dot{y}_2 \end{bmatrix} = \begin{bmatrix} -\varepsilon & 0 & 0 & 0 & 0 & 0 \\ -\alpha_1\bar{y}_1 & -\varepsilon & \beta_1 - \alpha_1\bar{u}_o & 0 & 0 & 0 \\ \alpha_1\bar{x}_1 & \alpha_1\bar{u}_o - \beta_1 & -\varepsilon & 0 & 0 & 0 \\ 0 & 0 & 0 & -\varepsilon & \gamma_1\bar{y}_1 & -\gamma_1\bar{x}_1 \\ 0 & 0 & 0 & 0 & -\varepsilon & \beta_2 - \alpha_2\bar{u}_o \\ 0 & 0 & 0 & 0 & \alpha_2\bar{u}_o - \beta_2 & -\varepsilon \end{bmatrix} \cdot \begin{bmatrix} \delta u_o \\ \delta x_1 \\ \delta y_1 \\ \delta z \\ \delta x_2 \\ \delta y_2 \end{bmatrix} \tag{29}$$

The eigenvalue equation is

$$(\varepsilon + \sigma)^2 \left((\varepsilon + \sigma)^2 + (\beta_1 - \alpha_1\bar{u}_o)^2 \right) \left((\varepsilon + \sigma)^2 + (\beta_2 - \alpha_2\bar{u}_o)^2\right) = 0 \tag{30}$$

where σ is the eigenvalue, which has the following six roots

$$\sigma_{1,2} = -\varepsilon \qquad \sigma_{3,4} = -\varepsilon \pm i(\beta_1 - \alpha_1\bar{u}_o) \quad \sigma_{5,6} = -\varepsilon \pm i(\beta_2 - \alpha_2\bar{u}_o)$$

The single steady state is thus always stable as all real parts of the eigenvalue are negative.

3.2.3 Combined forcing by orography and momentum sources/sinks

Combining orographic and momentum forcing, we get a steady state problem that has to be solved numerically. Using the same procedure as in the case where we only had orographic forcing, we may plot a graph of $\frac{u_{oE}}{\varepsilon}$ as a function of z with one branch for each u_o which is a real root of the equation $\dot{z} = 0$. For small values of momentum forcing in the wave components we obtain a graph which only differs slightly from Fig 6a, but as the amplitude of the forcing is increased, we obtain a bifurcation from one to three steady states even for mountain heights well below the critical one in Fig. 6a. The minimum forcing amplitude required in the wave components for a bifurcation to occur depends on the phase angle between the orography and the momentum forcing and the strength of the zonal momentum forcing.

Increasing the amplitude of the wave forcing further, we obtain three steady states over certain phase intervals and for large values of the momentum forcing, we have further bifurcations into more than three steady states. For a large momentum source/sink the physical validity of the model is very questionable, so here we have chosen to analyse a case where the forcing amplitude is just above the first bifurcation point and we have three steady states in two disconnected phase intervals. There is one interval around 0 degrees, that is, a vorticity sink in regions of orographic maxima, and one interval around 180 degrees which gives a vorticity source around orographic maxima. The bifurcation plots are shown in Figs. 7a and 7b for the intervals around 0^o and 180^o respectively.

A numerical investigation of the eigenvalues shows that the steady states corresponding to points on the bifurcation curves have stability properties as indicated by dashed (unstable) and full lines (stable) in Fig. 7.

For the parameter values chosen in Fig. 7, we see that there is quite a wide range of u_{oE} values for which there exist three steady states when the phase difference is around 0^o. It may also be seen that for a phase difference of 60^o, the $\frac{u_{oE}}{\varepsilon}$ value required for three steady states to occur is at a minimum. Around the 180^o bifurcation, the interval in $\frac{u_{oE}}{\varepsilon}$ is smaller and the minimum value of $\frac{u_{oE}}{\varepsilon}$ required is higher than in the earlier case. To exemplify the bifurcations occurring in the two different phase intervals, plots of the stream functions associated with each possible steady state for a given set of parameter values have been prepared (Fig. 8).

The most realistic flow patterns are obtained in an example where the phase difference is around 0^o. This corresponds to a winter type circulation where heating over oceans acts as a source of cyclonic vorticity. The intersections between the curve for 0^o phase difference and the horizontal line for

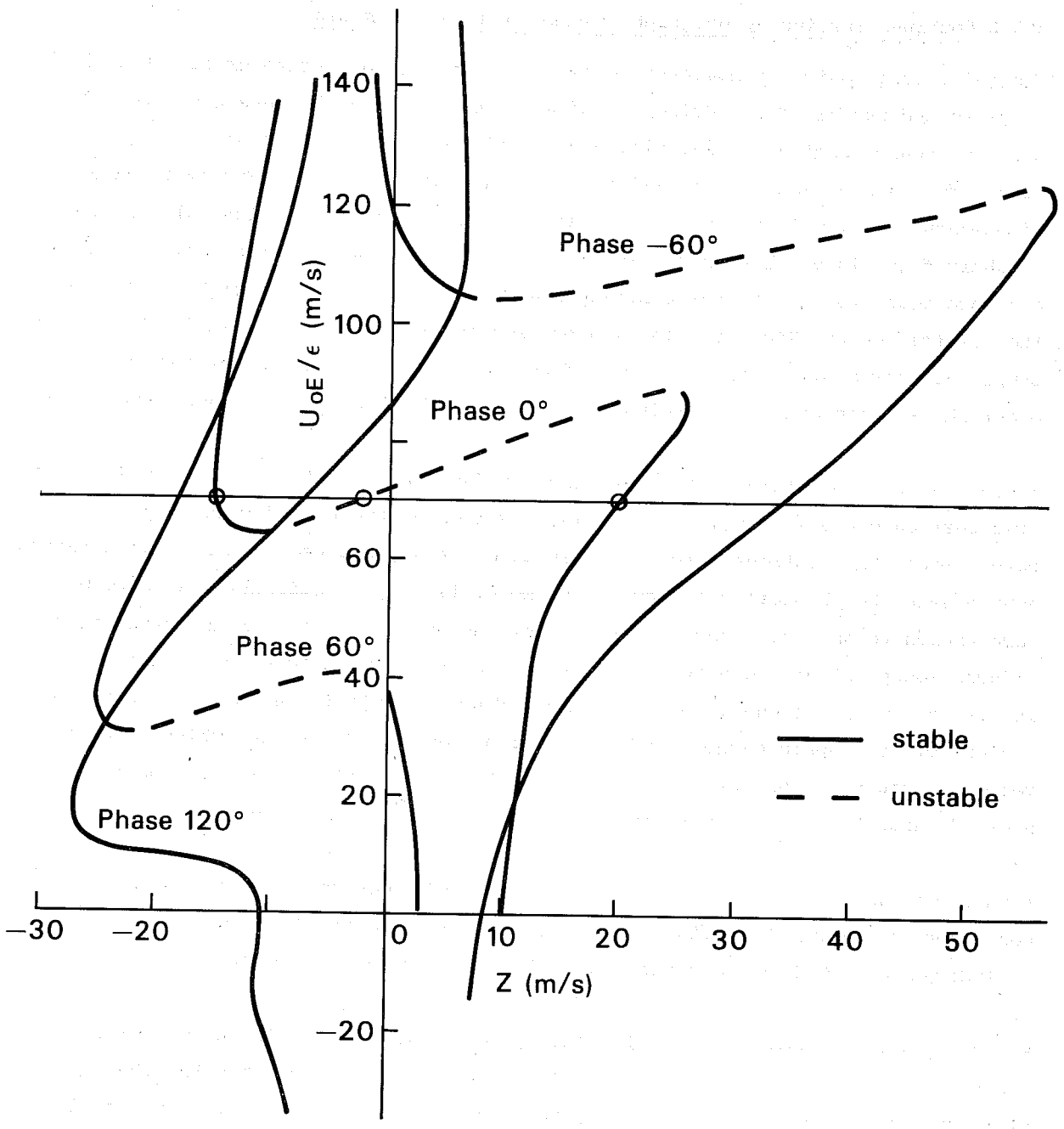

Fig. 7a Illustration of the bifurcation properties for the case of an asymmetric zonal component, z. Momentum forcing is present in the zonal component with amplitude u_{oE}, and the wave components with $\ell = 2$ and $n_1 = 3$ (amplitudes x_{1E} and y_{1E}). The axes are similar to the ones in Fig. 4, the only difference being that the horizontal axis here gives the steady state value of z. The wave forcing amplitude in terms of the linear response when no orography and no non-linearities are present

$$[(x_{1E}^2 + y_{1E}^2)/(\epsilon^2 + \beta_1^2)]^{\frac{1}{2}},$$

is 25 m/s (zonally averaged velocity at 45^o latitude).
The thin horizontal lines at $u_{oE}/\epsilon = 70$ m/s in both figures indicate which values are taken for the examples of Figs. 8-11.
Parameter values used: $\epsilon = 0.1$, $H = 8$ km, $\Omega = 7.29 \cdot 10^{-5}$ s^{-1}, $a = 6.37 \cdot 10^6$ m, $\mu_0 = 0.71$, $h_1 = 0.1$

Curves are given for a phase shift between the orographic and asymmetric momentum forcing ranging from -60^o to 120^o.

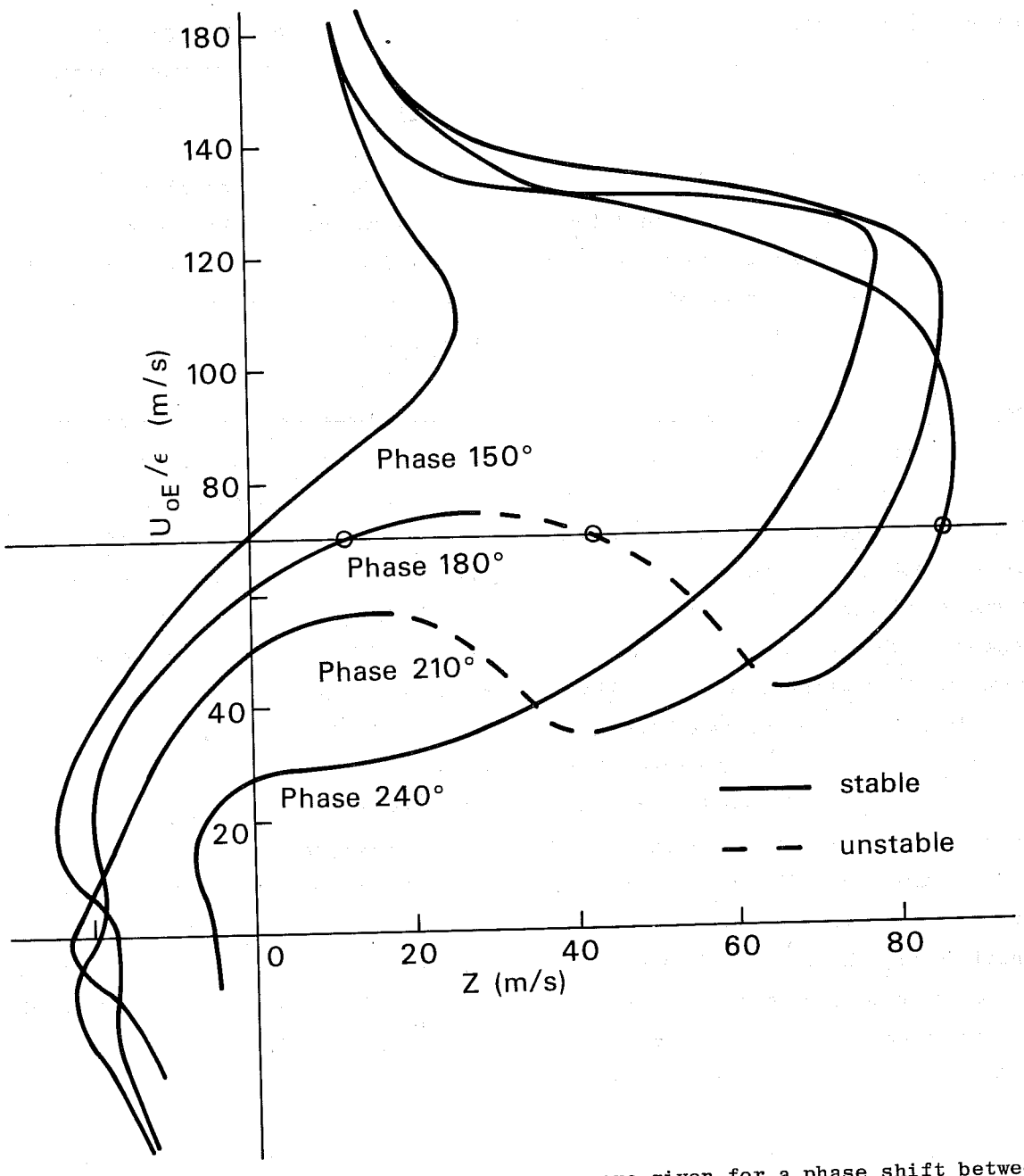

Fig. 7b Same as for Fig. 7a but here curves are given for a phase shift between the orographic and asymmetric momentum forcing ranging between 150° and 240°.

u_{oE}/ε = 70 m/s in Fig. 7a give the amplitudes of the z-component at the steady states. With the aid of Eqs. (26)-(27) we may calculate the amplitudes of the other components and the resulting stream function fields are shown in Fig. 8. The top and bottom flow fields are stable while the middle one is unstable. Comparing the two stable flow fields, one sees that the top one has a more pronounced wave component than the bottom one (due to the unequal spacing of the isolines for the stream function this is perhaps more evident when comparing the energetics given in Fig. 9). One may therefore associate the top flow field with a "blocked" situation while the bottom one, with the phase of the trough being much more to the east, may be thought of as a high index zonal type of circulation. The trough in the "blocked" state is roughly in phase with the trough found in the case where we had no momentum forcing in the wave components (Fig. 6b) while the trough of the unstable steady state is almost in phase with the trough found in the case with pure momentum forcing (Eq. 28).

Comparing the energetics of the two stable steady states (Fig. 9), one notices that the zonal state has a much higher value of the total kinetic energy than the blocked state, the difference being mostly in the zonal components. The direction of the energy flow between zonal and eddy kinetic energy caused by the orography is another significant difference between the two stable states. In the zonal state, energy is transferred from the eddy components to the zonal components through the aid of the orography and the high level of the zonal energy is thus maintained. From Fig. 8 it may also be seen that in this case there is a trough upstream of the orographic high and the mountain drag is therefore negative. In the blocked state, the orography acts to transfer energy in the other direction and the flow has arranged itself to pick up less energy from the momentum forcing. In this case the mountain drag is positive and thus the zonal flow over orography is generating waves. The efficiency of the two stable flows in converting the energy given by the momentum forcing into kinetic energy is thus different in the two stable cases. The difference arises due to the competing effects of the momentum forcing and the orography. Through the non-linearities of the system, this results in the possibility of having two different stable flow configurations.

The unstable steady state is mostly driven by pure momentum forcing. In this state the non-linear energy transfer is small and the wave is almost in phase with the orography thus making the mountain drag small. The state closely corresponds to the purely momentum forced steady state without mountains as given by Eq. (28).

In the case where we have a momentum forcing which is 180° out of phase with the orographic forcing, the difference between the two stable steady states is not as significant as in the previous case. The top stable state in Fig. 10 is one in which the trough generated by the momentum forcing and the lee trough of the mountain have merged while the zonal current is fairly weak. The bottom flow field is one in which the zonal current is stronger and the ridge over the low in the orography, or ocean part, is well developed.

The energetics for this case (Fig. 11) shows that the part of the kinetic energy transfer which is due to the orography is not very strong and its direction and intensity is very similar in all three steady states. The non-linear energy transfer due to flow-flow interactions, on the other hand, is in this case much more significant. In the top stable, steady state in Fig. 10 there is a fairly strong energy transfer by flow-flow interactions from eddy kinetic energy to zonal kinetic energy while the two other steady states have very weak flow-flow interactions and the energy transfer is in opposite directions. From the energetics, one may therefore draw the conclusion that the distinguishing feature of this bifurcation is not the orography but rather the non-linearities in the system giving rise to flow-flow interactions.

The physical significance of this case is not very clear as it corresponds to a situation with a strong cyclonic vorticity source over the continents and a strong zonal forcing. A cyclonic vorticity source over continents implies a strong heat source over continents compared to oceans and this is mostly the case during summers. Summer circulations are, however, weaker than winter circulations and they are, in particular, not characterised by a strong zonal forcing.

4. DISCUSSION AND CONCLUSIONS

It has been demonstrated that an extension of the β-plane model studied by CdV to a spherical geometry does give similar bifurcation properties even though the truncated equations are not the same due to the difference in geometry. If the low order model flow is confined to one hemisphere only, orographic forcing and zonal Newtonian forcing is not sufficient to force the model into multiple equilibria for realistic mountain heights and zonal windspeeds. However, a combination of mountains and zonally asymmetric momentum forcing may force the flow into two different stable equilibria, one predominantly zonal and the other with a more pronounced wave component. The phase and intensity of the asymmetric Newtonian forcing suggests that this corresponds to a wintertime circulation with strong heating over oceans and a fairly strong zonal flow. Examining the energetics of the two stable equilibria, one finds that in the zonal state, there is an energy transfer from the eddy components to the zonal flow through the effect of

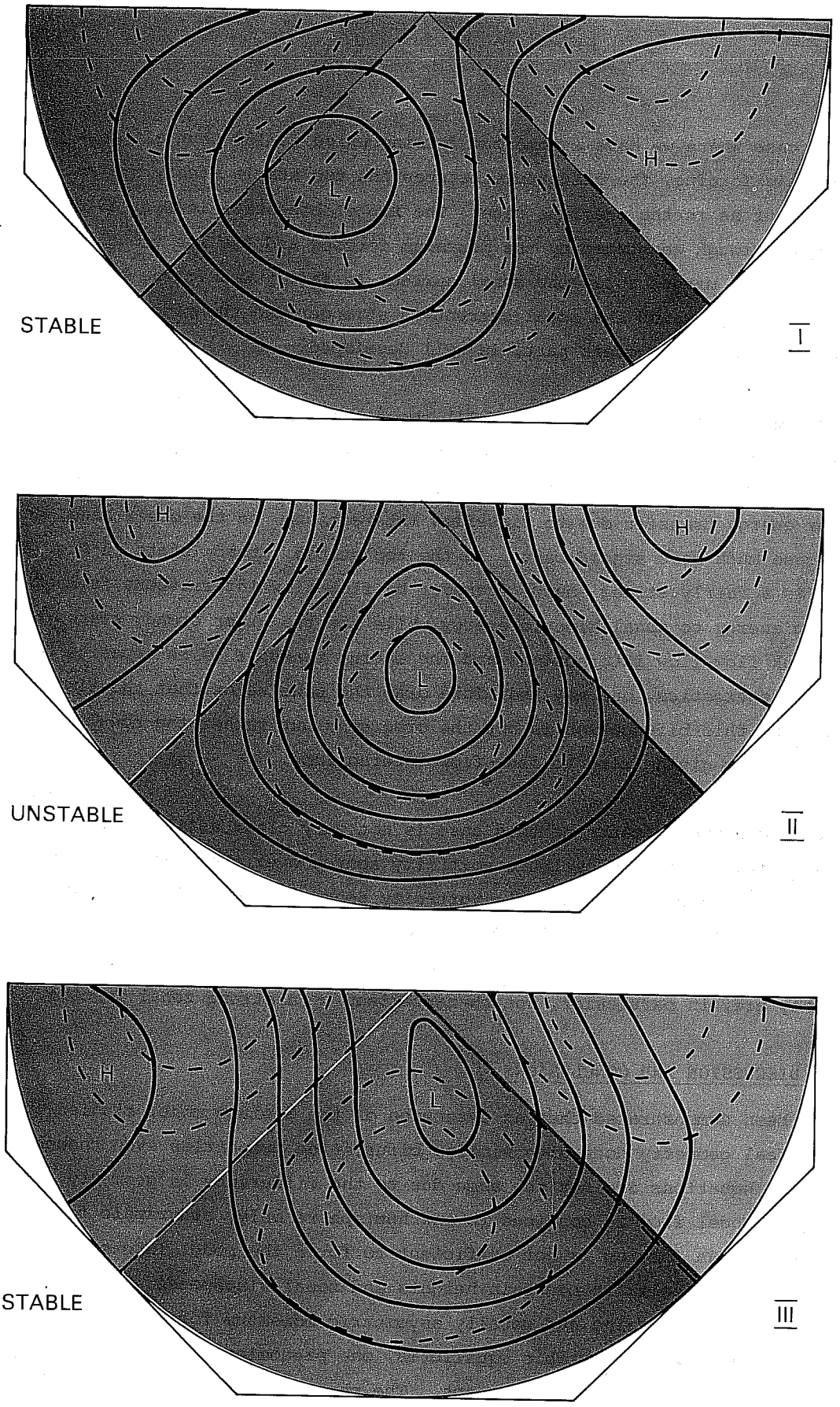

g. 8 Flow fields for the three equilibria obtained when the wave momentum forcing is in phase with the orography, which corresponds to vorticity sources over orographic lows. Full lines are isolines for the streamfunction, dashed lines are isolines for the orography. Please note that the differences between the isolines for the streamfunction are not the same in all three flow fields. Regions with the orography above its mean value ("land areas") are green, while areas with the orography below its mean value ("oceans") are blue. Parameter values are the same as in Fig. 7a, the three equilibria are those given by the intersections between the thin horizontal line at u_{oE}/ε = 70 m/s and the curve for phase 0^{o} in Fig. 7a.

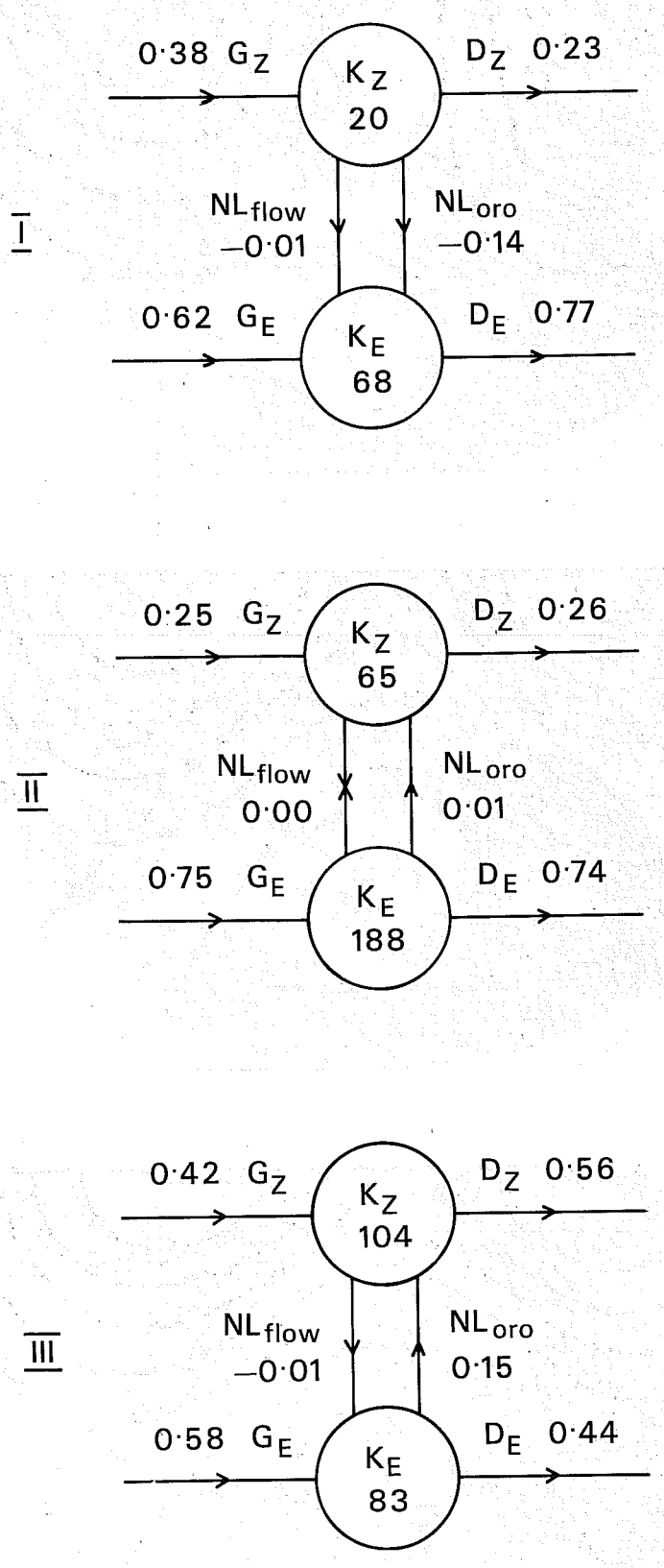

Fig. 9 Energetics of the three equilibria shown in Fig. 8. The total zonal and eddy kinetic energies are given in arbitrary energy units while the energy flows are normalized with the totally dissipated energy. For a description of the energy calculations, see Appendix II.

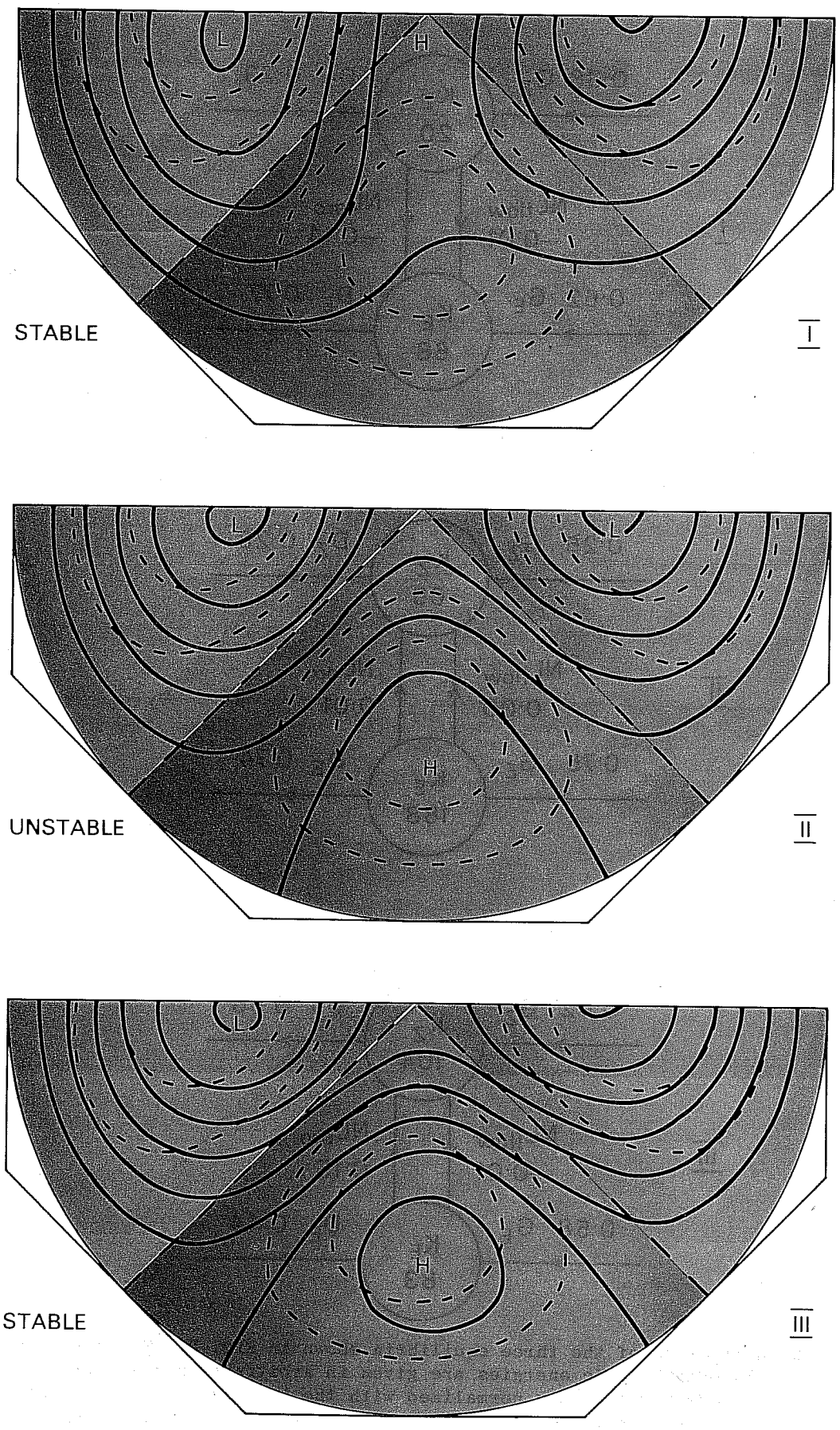

Fig. 10 Same as Fig. 8 but for a phase difference between orography and wave momentum forcing of 180^{o} (vorticity sources over orographic highs).

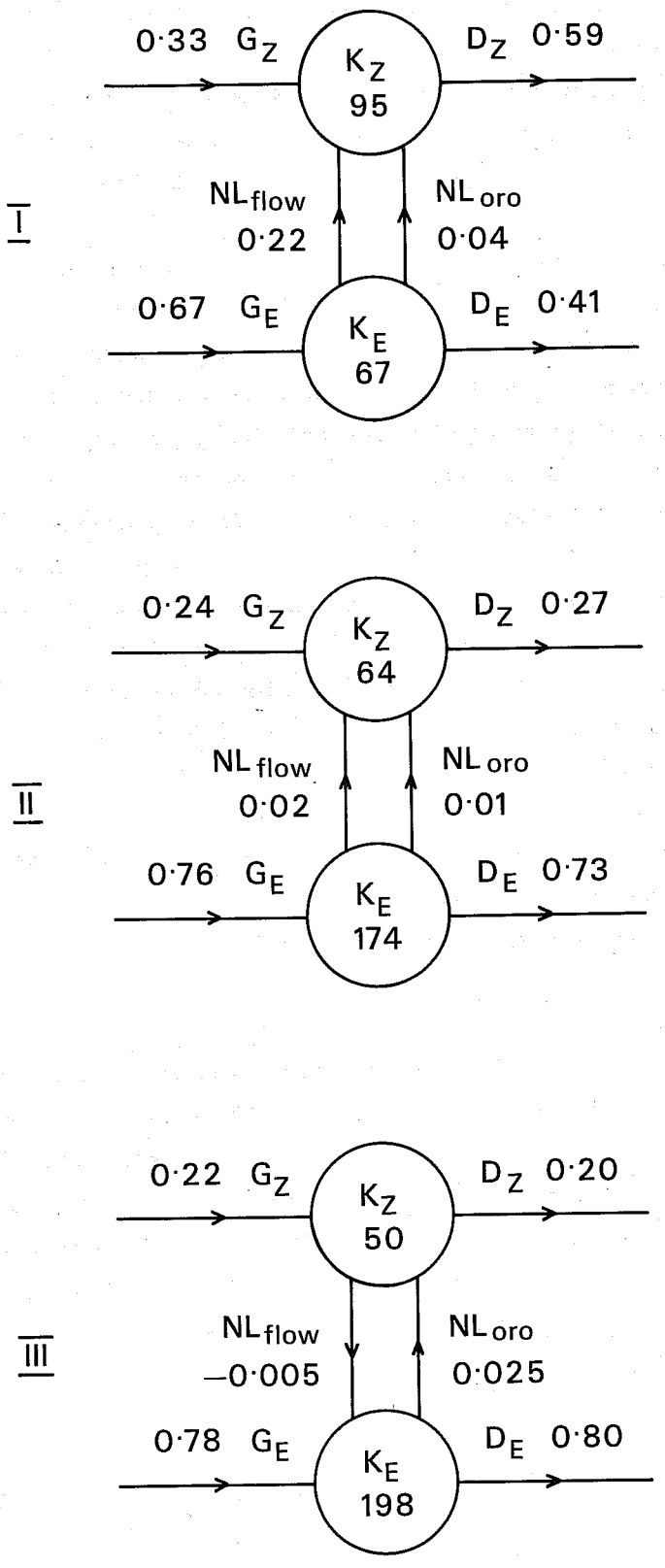

Fig. 11 Energetics of the flow fields shown in Fig. 10. For further explanations, see Fig. 9.

the orography, while the "blocked" state has an energy transfer in the other direction. In the unstable steady state, the non-linear energy transfer is fairly weak. The orography may thus be seen to act as a triggering mechanism, directing the basically Newtonianly forced flow into one or the other of the stable states when the Newtonian forcing exceeds a certain critical value. Comparing this mechanism to reality, one may reason as follows:

When the asymmetric heating is weak, the large-scale flow has only one possible equilibrium state but, as heating over oceans and cooling over land areas increases from autumn to winter, the atmosphere is driven into one of the two stable and totally different flow types. Which one it chooses is crucially dependent upon the initial state of the flow and the way in which the forcing is changing in time. Once the atmosphere has reached the "attractor basin" of one of the stable states, it stays there until the forcing changes to drive it away into some other "attractor basin". The predictability of the atmosphere is thus low when the forcing is just above the critical value for a bifurcation to occur, but once the flow has settled itself into one of the attractor basins, the predictability increases. In the case of a blocked situation over the eastern Atlantic Ocean, this feature has indeed been observed (Bengtsson, 1980) with a numerical prediction model.

A comparison of the energetics derived for the two stable states (Fig. 9) in the 0^{o} case with reality can be made through the studies by Wiin Nielsen et al (1964, 1965). They examined Northern Hemisphere data for two winter months, January 1962 and 1963.

Fig. 12 shows the time averaged 700 mb circulation over the N. American - Atlantic - W. Europe area for the two Januarys and the energetics taken from Wiin-Nielsen (1965). January 1962 was a typical winter month with a predominantly zonal circulation and the energetics show an energy transfer taking place from the eddy to the zonal kinetic energy. January 1963, on the other hand, was a typically "blocked" month with a stronger eddy flow and a kinetic energy transfer from the zonal to the eddy kinetic energy. In Wiin-Nielsen et al (1964) it was also shown that the reversal of the energy transfer in January 1963 mostly took place in wavenumbers two and three.

Whether this is due to the orography or not is an open question but there is a striking similarity in the energetics between the observational study by Wiin-Nielsen et al and the results obtained here for a low order barotropic model with orographic and Newtonian forcing.

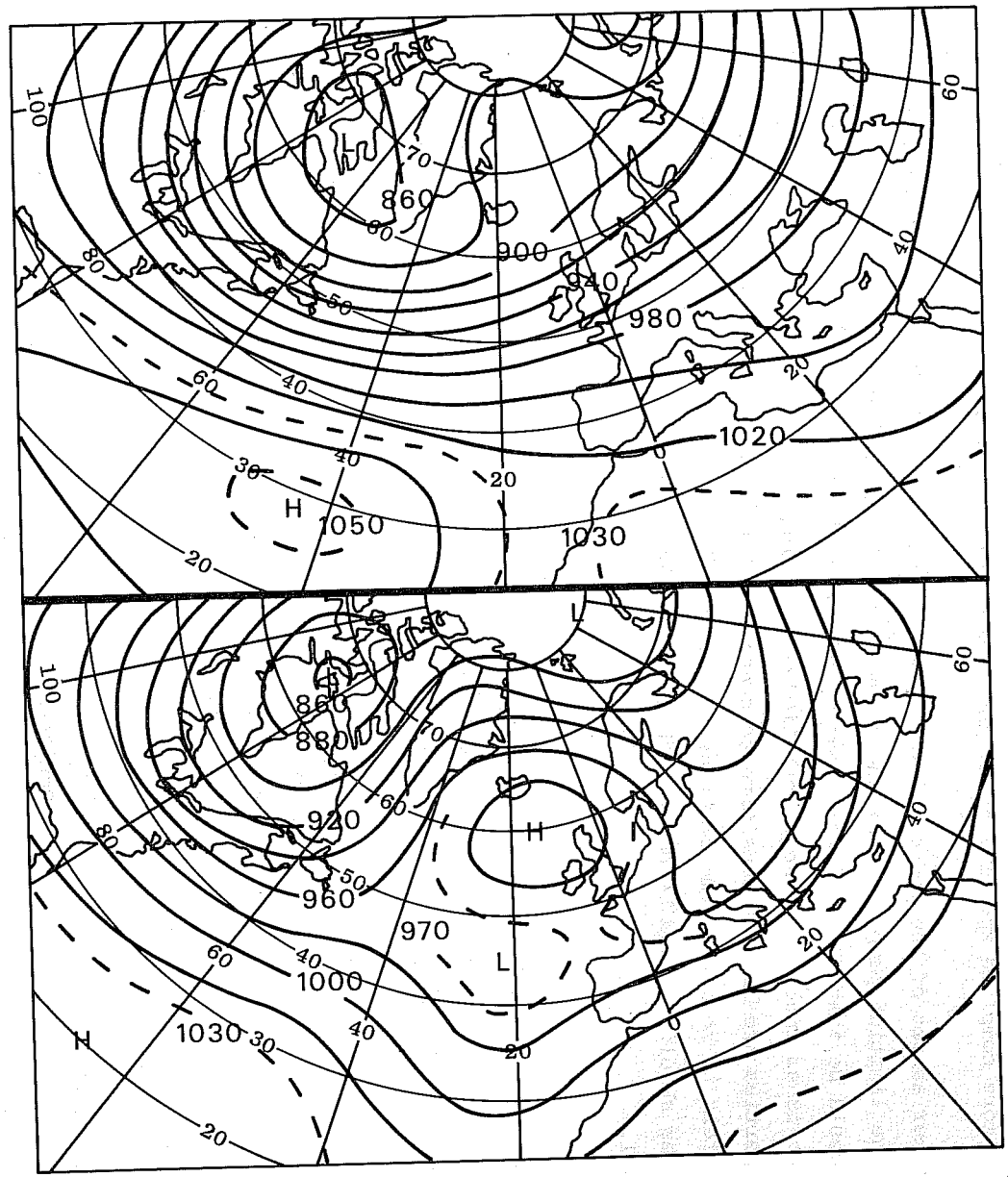

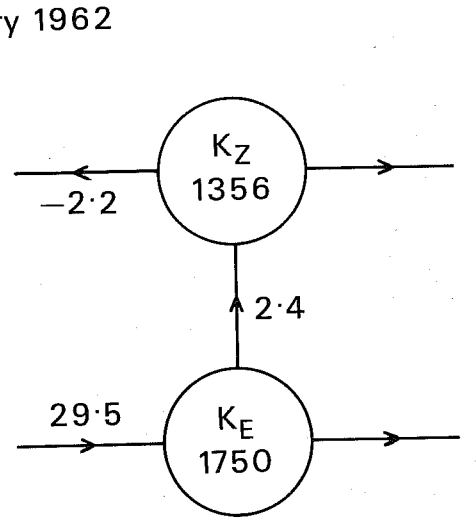

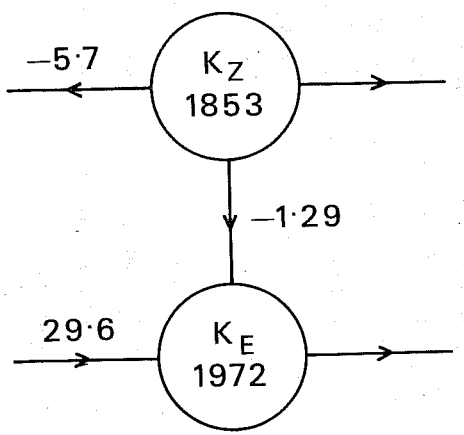

Fig. 12 Energetics and 700 mb flow fields given as monthly averages for January 1962 and January 1963. Height contours are given in tens of feet. The maps are redrawn from Stark (1962) and O'Connor (1963). The energetics are calculated from observations and the values are taken from Wiin-Nielsen (1965). The kinetic energy in each box is in units of kJm^{-2}, energy flows are in units of 10^{-4} $kJm^{-2}s^{-1}$.

In the case of a Newtonian forcing 180° out of phase with the orography (Fig. 10 and 11) it has not been possible to find observational studies verifying the model results. This is most probably due to the fact that during summers the zonally asymmetric heating is weaker (Ashe 1979) and the bifurcation into multiple equilibria is therefore not as clearly marked as in the winter case. It is also well known that the zonal circulation is not very intense during summers and the importance of the large-scale orography for the ultra-long waves thus decreases.

The comparison of results from this simple model with observations should, of course, not be taken too seriously. The main purpose of this study is to examine a plausible physical mechanism acting through the non-linearities of the governing equation. The main shortcoming of the simple model is the severe truncation.

In the paper by CdV, it was however demonstrated that in a grid point model with many more degrees of freedom, the stable equilibria found in the truncated spectral model still existed. A natural continuation of this study is therefore also to investigate numerically the possible existence of multiple steady states in a more complete spectral model and this is planned to be done.

Another aspect of the low order model, which has not at all been dealt with here, is the limiting properties of the trajectories in the six-dimensional phase space. It could be that the "attractor basin" of one of the stable steady states in phase space is so small that the probability of reaching it is very low. The limiting properties are however sensitive to changes in the truncations and it is therefore not felt to be a very important aspect of this low order model. The limiting properties should instead be dealt with in connection with the more complete spectral model.

If the orography acts as a triggering mechanism, directing the flow into one or the other of the stable steady states, it should be possible to find this in observational data by evaluation of the term $J(\psi,h)$ and its contribution to the energy transfer between eddy and zonal kinetic energy. One would have to find some objective method of defining a "blocked" and a "zonal" state to divide the data into distinct groups and then examine the energetics of each group. Preferably this data study should be made on a limited area to more easily identify the blocking situation, the heating contrasts land/ocean and the orographic effects. It is planned that a study of this type will be performed with data available at ECMWF.

Acknowledgements

I would like to thank Drs. L. Bengtsson, J. Derome and A. Wiin-Nielsen for many useful discussions and comments. Dr. H. Sundquist has been most helpful in suggesting changes to improve the readability of the manuscript.

References

Ashe, S., 1979 A nonlinear model of the time-average axially asymmetric flow induced by topography and diabatic heating. J.Atmos.Sci., 36, 109-126.

Bengtsson, L., 1980 Numerical prediction of atmospheric blocking - A case study. Accepted for publication in Tellus.

Charney, J.G. and De Vore, J.G., 1979 Multiple flow equilibria in the atmosphere and blocking. J.Atmos.Sci., 36, 1205-1216.

Kalnay-Rivas, E. and Merkine, L.-O., 1980 A simple mechanism for blocking. Submitted for publication.

Lorenz, E.N., 1960 Maximum simplification of the dynamic equations. Tellus, 12, 243-254.

Lorenz, E.N., 1962 Simplified dynamic equations applied to the rotating-basin experiments. J.Atmos.Sci., 19, 39-51.

O'Connor, J.F., 1963 The weather and circulation of January 1963. Mon.Wea.Rev., 91, 209-218.

Platzmann , G.W., 1962 The analytical dynamics of the spectral vorticity equation. J.Atmos.Sci., 19, 313-328.

Stark, L.P., 1962 The weather and circulation of January 1962. Mon.Wea.Rev., 90, 167-174.

Trevisan, A. and Buzzi, A., 1980 Stationary response of barotropic weakly non-linear Rossby waves to quasi-resonant orographic forcing. Accepted for publication in J.Atmos.Sci.

Wiin-Nielsen, A., Brown, J.A. and Drake, M., 1964 Further studies of energy exchange between the zonal flow and the eddies. Tellus, 16, 168-180.

Wiin-Nielsen, A., 1965 Some new observational studies of energy and energy transformations in the atmosphere, WMO Technical Note No. 66, No. 162 TP. 79, Geneva, Switzerland, 177-202.

Wiin-Nielsen, A., 1979 Steady states and stability properties of a low order barotropic system with forcing and dissipation, Tellus, 31, 375-386.

APPENDIX I

LIST OF SYMBOLS

η	dimensional streamfunction
η_E	dimensional forcing streamfunction
$\underline{V}$	dimensional wind vector
t	dimensional time
f	Coriolis parameter ($2\Omega\mu$)
ω	$\frac{dp}{dt}$
p	pressure
p_o	surface pressure
E	dimensional dissipation coefficient
w	vertical velocity
g	acceleration of gravity
ρ_o	density of assumed isothermal atmosphere
m	dimensional mountain height
H	scale height of the atmosphere $(\frac{p_o}{g\rho_o})$
Ω	angular velocity of the earth
a	radius of the earth
τ	non-dimensional time
ψ	non-dimensional streamfunction
ζ	non-dimensional vorticity
ζ_E	non-dimensional vorticity forcing
ϵ	non-dimensional dissipation rate
μ	$\sin\phi$, where ϕ is latitude
λ	longitude

APPENDIX II

ENERGY CALCULATIONS

The energetics of the steady states, as shown in Figs. 9 and 11, are calculated in the following way:

Total zonal kinetic energy $K_z = 2(2u_o^2 + cz^2)$

Total eddy kinetic energy $K_E = c_1(x_1^2 + y_1^2) + c_2(x_2^2 + y_2^2)$

Generation of zonal kinetic energy $G_z = 4u_o u_{oE}$

Generation of eddy kinetic energy $G_E = c_1(x_{1E}x_1 + y_{1E}y_1)$

Dissipation of zonal kinetic energy $D_z = -\varepsilon K_z$

Dissipation of eddy kinetic energy $D_E = -\varepsilon K_E$

Energy transfer between zonal and eddy kinetic energies induced by orography, $NL_{oro} = 2h_1 [y_1(2\delta_1 u_o - c\delta_3 z) - y_2 c\delta_2 z]$

The non-linear energy transfer due to flow-flow interactions (NL_{flow}) is calculated as a residual.

ECMWF PUBLISHED TECHNICAL REPORTS

No.1 A Case Study of a Ten Day Prediction

No.2 The Effect of Arithmetic Precisions on some Meteorological Integrations

No.3 Mixed-Radix Fast Fourier Transforms without Reordering

No.4 A Model for Medium-Range Weather Forecasting - Adiabatic Formulation

No.5 A Study of Some Parameterizations of Sub-Grid Processes in a Baroclinic Wave in a Two-Dimensional Model

No.6 The ECMWF Analysis and Data Assimilation Scheme - Analysis of Mass and Wind Fields

No.7 A Ten Day High Resolution Non-Adiabatic Spectral Integration: A Comparative Study

No.8 On the Asymptotic Behaviour of Simple Stochastic-Dynamic Systems

No.9 On Balance Requirements as Initial Conditions

No.10 ECMWF Model - Parameterization of Sub-Grid Processes

No.11 Normal Mode Initialization for a Multi-Level Gridpoint Model

No.12 Data Assimilation Experiments

No.13 Comparison of Medium Range Forecasts made with two Parameterization Schemes

No.14 On Initial Conditions for Non-Hydrostatic Models

No.15 Adiabatic Formulation and Organization of ECMWF's Spectral Model

No.16 Model Studies of a Developing Boundary Layer over the Ocean

No.17 The Response of a Global Barotropic Model to Forcing by Large-Scale Orography

No.18 Confidence Limits for Verification and Energetics Studies

No.19 A low order barotropic model on the sphere with orographic and Newtonian forcing